ever, knockdown of EXOSC4 or EXOSC5 showed a marginal effect on VSV replication (Fig. 5E), at least under our experimental conditions. We do not exclude the possibility that knockdown of EXOSC4 or EXOSC5 is not an efficient method by which to reduce the antivirus role of the RNA exosome. Unexpectedly, the physical interaction between EXOSC4 and DDX60 was reduced after VSV infection (Fig. 5F).

We next examined the antiviral activity of DDX60. Interestingly, DDX60 overexpression suppressed the CPE induced by VSV infection and reduced VSV replication in HEK293 and HeLa cells (Fig. 6A to D). The suppression induced by DDX60 overexpression was observed even in EXOSC5 knockdown cells (Fig. 6B). PV replication was also suppressed by overexpression of DDX60 (Fig. 6E). Next, we performed a knockdown assay using shRNA for DDX60, which reduced expression of DDX60 mRNA and protein (Fig. 6F) (see also Fig. 11 and 12). Unlike the results seen with EXOSC4 and EXOSC5, knockdown of DDX60 increased VSV replication and enhanced CPE and did not inhibit cell growth (Fig. 5D and Fig. 6G and H). Because the interaction between DDX60 and the RNA exosome core component was reduced after viral infection, we examined the molecular mechanism by which DDX60 suppresses viral replication.

DDX60 associates with RIG-I-like receptors. To identify the antiviral pathway in which DDX60 is involved, we used immunoprecipitation assays to search for the protein that binds to DDX60. Because the RLR-dependent pathway plays an important role in the antiviral activity of the host cell, we examined the binding of DDX60 to proteins involved in this pathway. Interestingly, DDX60 was coimmunoprecipitated with RIG-I, MDA5, and LGP2 but not with IPS-1 or IKK-ε, which are downstream factors of RIG-I and MDA5 (Fig. 7A). RNase A or RNase III treatment did not abolish the interaction between DDX60 and RIG-I or MDA5 (Fig. 7B and C), indicating that these associations are not mediated via RNA. DDX60 did not bind to HMGB1 before or after dsRNA stimulation or VSV infection (Fig. 7D). To further confirm the binding of DDX60 to RIG-I, we examined the interaction of DDX60 with endogenous RIG-I by the use of anti-RIG-I monoclonal antibody. RIG-I mRNA levels are known to increase after viral infection (59). We observed an increase in RIG-I protein levels after poly(I · C) stimulation (data not shown). However, the protein level in HEK293FT cells was not increased after VSV infection in our experiment for unknown reasons (Fig. 7E). Endogenous RIG-I was found to interact with DDX60 after VSV infection but not in its absence (Fig. 7E), indicating that interaction between DDX60 and endogenous RIG-I is dependent on viral infection, although the interaction between overexpressed RIG-I and DDX60 was independent of viral infection.

Next, we used confocal microscopy to examine the intracellular colocalization of DDX60 with RIG-I and MDA5. Consistent with the immunoprecipitation assay, confocal microscopic analysis showed that DDX60 was partially colocalized with overexpressed RIG-I and MDA5 before and after VSV infection or poly(I · C) stimulation (Fig. 7F and G). We tried to observe endogenous RIG-I by confocal microscopy; however, we could not detect endogenous RIG-I in our tests for technical reasons. We also used RIG-I partial fragments to identify the region of RIG-I that binds to DDX60 (Fig. 7H). RIG-IC, which includes a helicase domain and CTD, was coimmunoprecipitated with DDX60, while the N-terminal CARD of RIG-I was not (Fig. 7H). These data indicate that DDX60 binds to the RIG-IC fragment.

The DDX60 helicase domain binds to viral RNA. In light of the binding of DDX60 to viral RNA sensors RIG-I and MDA5, we hypothesized that the RNA helicase domain of DDX60 binds to viral RNA. To test this hypothesis, we expressed a histidine-tagged DDX60 RNA helicase domain (aa 752 to 1337) in *E. coli* (Fig. 8A). The protein was purified using nickel-nitrilotriacetic acid (Ni-NTA) resin, analyzed by SDS-PAGE, and stained with CBB. Protein purity was found to be greater than 90% (Fig. 8B). VSV single- and double-stranded RNA was synthesized *in vitro*. Binding of the DDX60 helicase domain to *in vitro*-synthesized viral RNA was examined using gel-shift assays. Single- or double-stranded VSV RNA mobility was found to decrease as a result of the addition of DDX60 helicase (Fig. 8C and D). DDX60 was also found to bind to dsRNA treated with alkaline phosphatase, suggesting that the presence of 5′ triphosphate is nonessential for this binding (Fig. 8E). The mobility shift of ssRNA was different from that of dsRNA; this difference might have been a result of the stoichiometry assays. Interestingly, dsDNA was also shifted in the presence of DDX60 protein (Fig. 8F). As a control we used DDX6, a DEXD/H box RNA helicase distantly related to DDX60. DDX6 also bound to ssRNA (Fig. 8C); however, DDX6 only minimally reduced the mobility of dsRNA and dsDNA compared to DDX60 (Fig. 8D and F).

DDX60 promotes RIG-I- or MDA5-dependent expression of type I IFN. Next, we examined whether DDX60 is involved in RIG-I- or MDA5-mediated signaling. The prepared poly(I · C) solution contains various lengths of poly(I · C), both shorter and longer than 1 kbp (data not shown), in a mixture known to activate both RIG-I and MDA5 (20). Both RIG-I-mediated and MDA5-mediated IFN-β promoter activation by poly(I · C) transfection were enhanced by DDX60 expression (Fig. 9A and B). As a control we used DDX6, a helicase distantly related to DDX60. Expression of DDX6 produced neither a positive nor a negative effect on the RIG-I-dependent IFN-β promoter activation (Fig. 9C). To address the function of the DDX60 helicase domain, we introduced the mutation (K791A) on the Walker type ATP binding site, which is essential for ATPase activity of RNA helicase (50). The mutation reduced the enhancement of RIG-I-mediated IFN-β promoter activation by DDX60 (Fig. 9C). Knockdown analysis using shRNA for DDX60 showed that IFN-β promoter activation by viral dsRNA was reduced in DDX60 knockdown cells compared with control cells (Fig. 9D). To exclude the off-target effect, we also used siRNA for DDX60, whose target sequence is different from that of shRNA for DDX60. Expression of DDX60 was efficiently reduced by siRNA for DDX60, and the siRNA for DDX60 efficiently reduced IFN-β mRNA expression by poly(I · C) stimulation (Fig. 9E to G). These knockdown results are consistent with the overexpression results described above, providing further evidence that DDX60 promotes RLR-mediated IFN-β expression.

In contrast, TICAM-1- and TLR3-mediated IFN-β promoter activation was not increased by overexpression of DDX60 (Fig. 9H and I). In addition, poly(I · C) stimulation of TLR3 without transfection resulted in normal expression

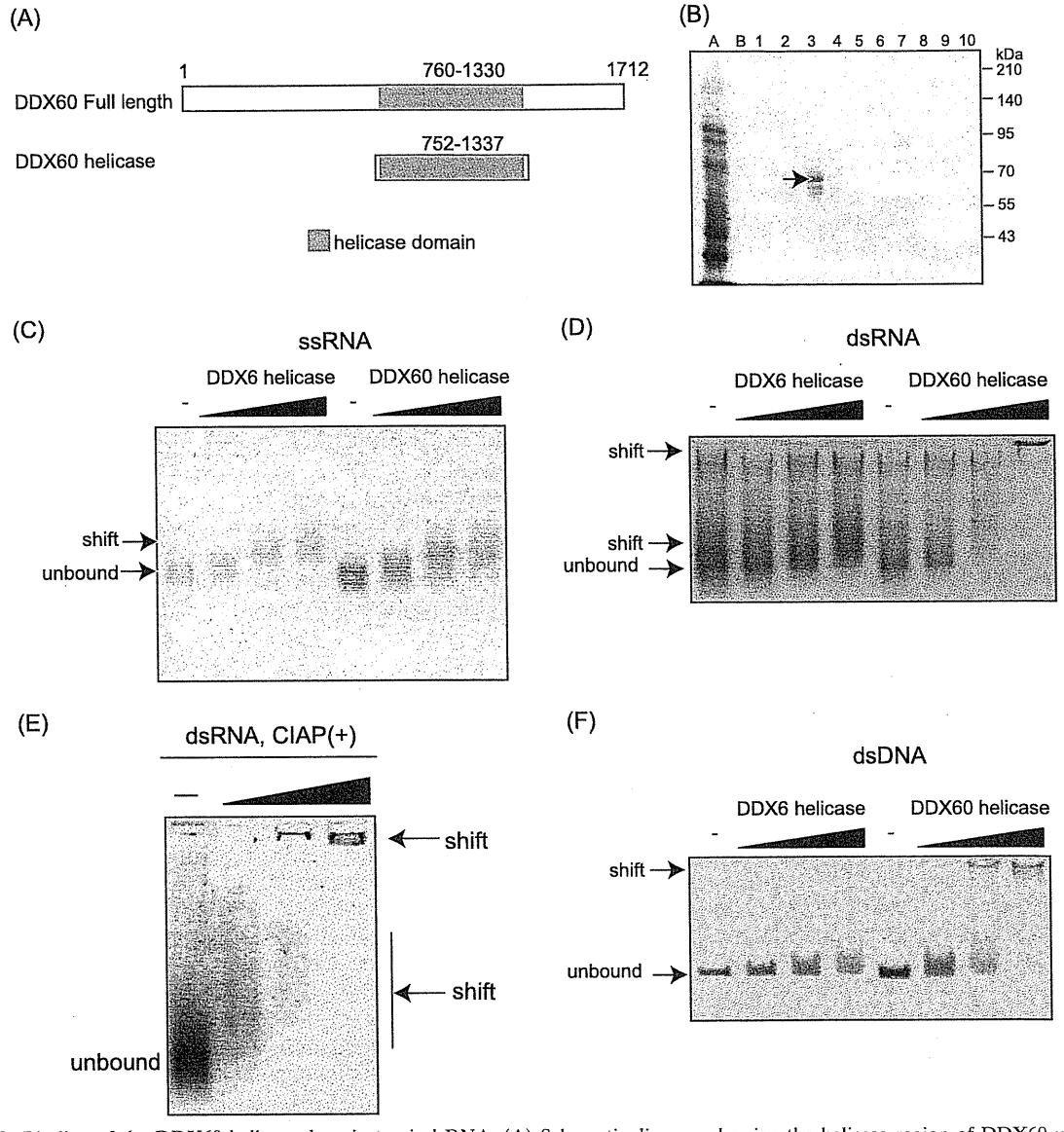

FIG. 8. Binding of the DDX60 helicase domain to viral RNA. (A) Schematic diagram showing the helicase region of DDX60 used for the following gel shift assay. (B) A His-tagged DDX60 helicase fragment was expressed in *E. coli* and purified using Ni-NTA resin. Purified products were analyzed by SDS-PAGE and stained with CBB. Lane A represents the nonabsorbed fraction, lane B represents the wash fraction, and lanes 1 to 10 represent the eluted fractions. The lane 3 fraction contains DDX60 protein. (C to F) Purified DDX60 and DDX6 fragments were incubated with *in vitro*-synthesized VSV ssRNA (C), dsRNA (D), dsRNA treated with calf intestinal alkaline phosphatase (CIAP) (E), or dsDNA (F), and the products were analyzed using agarose gel. The gel was stained with ethidium bromide.

of IFN-β in DDX60 knockdown cells (Fig. 9J). These data suggest that DDX60 is specific to the RLR pathway. Because the knockdown of EXOSC4 or EXOSC5 did not reduce the promoter activation resulting from VSV infection or dsRNA transfection (Fig. 9K and L), the data suggest that these proteins do not play a major role in DDX60-mediated enhancement of RIG-I or MDA5 signaling, at least under our experimental conditions. We also assessed the effect of DDX60 knockdown on IFN-β promoter activation by overexpressing TBK1, IPS-1, RIG-I CARDs, or MDA5 to discover the step at which DDX60 plays a role in RIG-I-mediated signaling. All of these procedures led to autoactivation, inducing transcription from the IFN-β promoter in the absence of RIG-I or MDA5 ligands (22). Although DDX60 knockdown reduces the IFN-β promoter activation induced by dsRNA transfection, it was not found to affect this autoactivation (Fig. 9M and N). These data suggest that shRNA suppression of DDX60 occurs upstream of RIG-I and MDA5 (Fig. 9O).

To examine the effect of DDX60 on the binding of RIG-I to dsRNA, we performed pulldown assays. The proteins were exogenously expressed in HEK293FT cells, and the proteins were recovered from cell lysates by the use of biotin-conjugated dsRNA and streptavidin Sepharose. RIG-I or DDX60 protein was recovered from cell extracts, suggesting the bind-

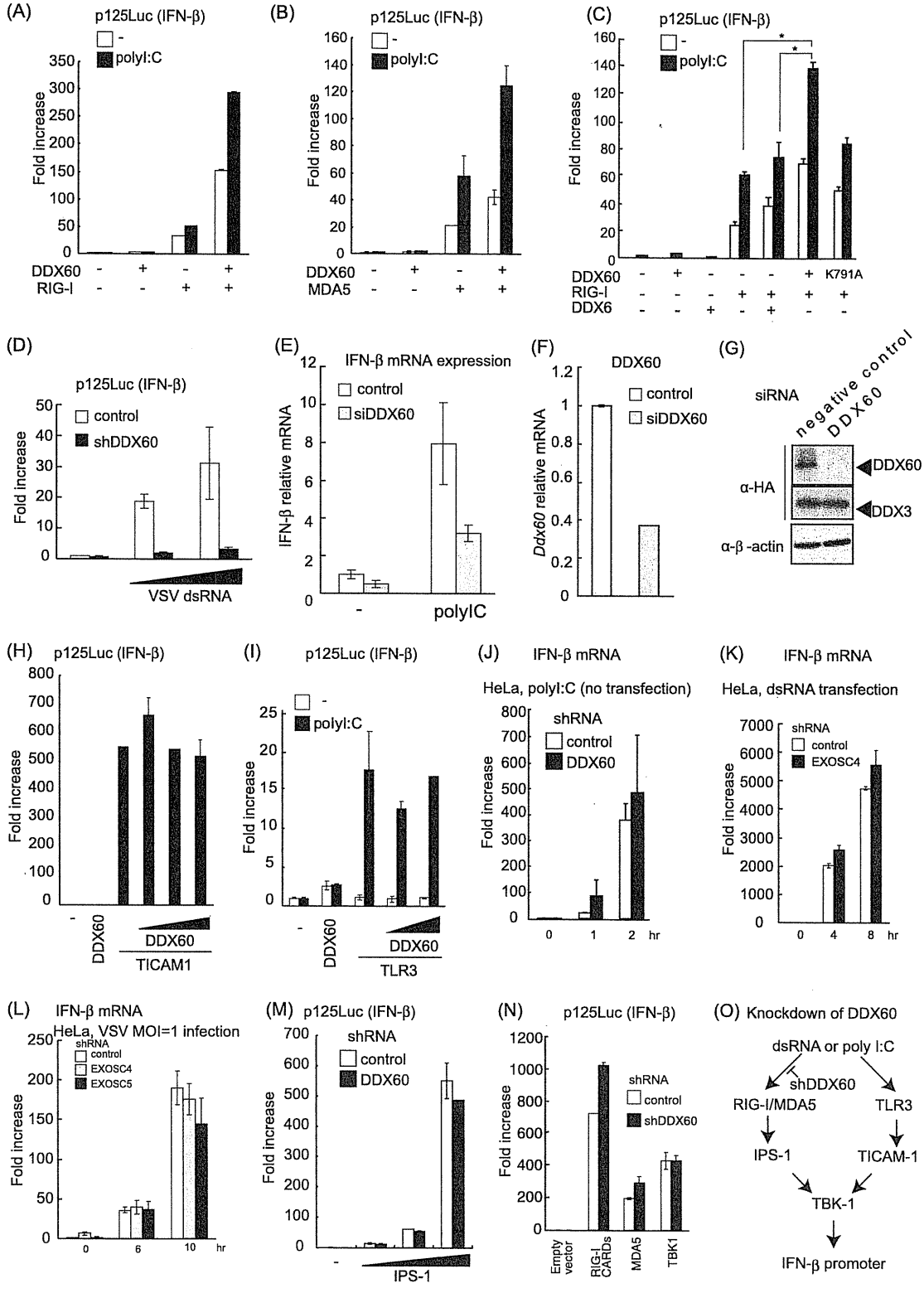

FIG. 9. DDX60 promotes RIG-I- or MDA5-mediated signaling. (A to C) Activation of the IFN-β promoter was examined using a reporter gene assay and p125luc plasmid. Vectors expressing RIG-I (A), MDA5 (B), DDX6 (C), and the wild type (WT) or DDX60-K791A (C) were transfected into HEK293 cells together with the reporter plasmid and *Renilla* luciferase plasmid (internal control). After 24 h, the cells were left unstimulated or stimulated with poly(I · C) by the use of DEAE-dextran for 4 h. Cell lysates were prepared, and luciferase activity was measured. (D) Control or DDX60 knockdown HEK293 cells were transfected with the p125luc reporter, *Renilla* luciferase plasmid, and/or *in vitro*-synthesized VSV

ing of RIG-I or DDX60 to dsRNA. Because both RIG-I and DDX60 can bind to dsRNA, the data do not imply an interaction between RIG-I and DDX60. Interestingly, coexpression of both proteins increased the levels of proteins recovered from the cell lysate (Fig. 10).

DDX60 is important for expression of type I IFN and IFN-inducible genes during viral infection. We next tested whether DDX60 is involved in cytokine expression during viral infection. RIG-I recognizes VSV and SeV, and MDA5 recognizes PV (3, 21). Interestingly, knockdown of DDX60 reduced IFN-β expression in HeLa cells after VSV, PV, and SeV infection. IFIT-1 and IP10 expression after VSV and SeV infection was also reduced by DDX60 knockdown (Fig. 11). Knockdown of DDX60 caused a marginal effect on expression of IFIT1 and IP10 in response to PV infection. Some of the IFN-α gene expression induced by other sensor molecules might have been responsible for the difference. Unlike viral infection, knockdown of DDX60 did not reduce expression of IFIT1 after IFN-β stimulation (Fig. 12A). Reduction of type I IFN expression was also observed after VSV infection in HEK293 cells (Fig. 12B and C). In addition, DDX60 knockdown reduced IRF-3 dimerization after VSV infection (Fig. 12D). These data indicate that DDX60 is required for RIG-I- and MDA5-dependent type I IFN and IFN-inducible gene expression during viral infection. We also observed that suppression of CPE and viral titers in culture medium induced by DDX60 overexpression can be reduced by IPS-1 knockdown (Fig. 6I and J), confirming that the antiviral activity of DDX60 is dependent on the presence of RLRs. Because the DDX60 helicase domain was found to bind to dsDNA, we examined whether DDX60 is involved in type I IFN expression after infection with HSV-1, a DNA virus. In this case, knockdown of DDX60 reduced expression of IFN-β and IP10 after HSV-1 infection (Fig. 12E and F).

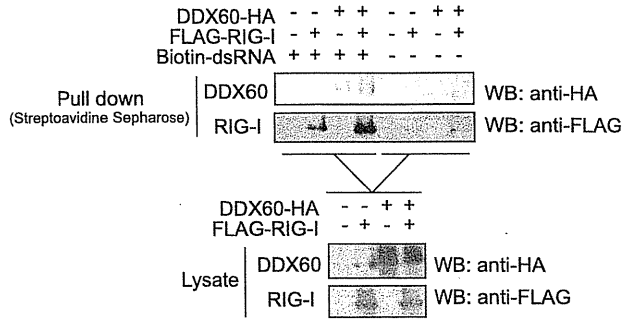

FIG. 10. DDX60 increases the association of RIG-I to short synthetic dsRNA. DDX60- and RIG-I-expressing vectors were transfected into HEK293FT cells. At 24 h later, cell lysate was prepared. The lysate was incubated with or without biotin-conjugated dsRNA, and the dsRNA was recovered using streptavidin Sepharose beads. The recovered fraction was analyzed by Western blotting.

DISCUSSION

Here, we report that DDX60 is a novel antiviral factor in human cells. The amino acid sequence of DDX60 is similar to that of Ski2 homologs, which are cofactors of the RNA exosome. DDX60 interacts with core components of the RNA exosome. After viral infection, the DDX60 protein binds to endogenous RIG-I protein and is involved in RIG-I-dependent pathway. The protein also binds to MDA5 and LGP2. The DDX60 helicase domain binds to viral RNA and DNA, and coexpression of RIG-I with DDX60 increases the binding of RIG-I and DDX60 to dsRNA. Knockdown of DDX60 reduces expression of type I IFN and IFN-inducible genes after VSV, PV, SeV, and HSV-1 infections. Therefore, we concluded that DDX60 is a novel antiviral helicase involved in RLR-dependent pathways.

Schröder et al. and Soulat et al. first reported that the non-RLR helicase DDX3 plays pivotal roles in RLR-dependent pathways (41, 43). DDX3 is ubiquitously expressed in a variety of cells and exerts its positive effect as a part of TBK-1- and/or IKK-ε-containing complexes that activate IRF-3 (41). DDX3 also binds to RIG-I and IPS-1 and promotes the activation of those proteins (28, 32). Our study showed that another non-RLR helicase, DDX60, is also involved in RLR-dependent pathways. Thus, our reports and previous studies demonstrate the important roles of non-RLR helicases in RLR-mediated signaling and antiviral response.

Because DDX60 protein does not contain CARDs, which are required for the interaction with IPS-1, it seems unlikely that DDX60 directly activates IPS-1 without RLRs. The results of knockdown studies suggest that DDX60 is an upstream factor of IPS-1, and the immunoprecipitation assay results suggest that DDX60 binds to the RLR upstream factors. On the basis of these findings, we expected that DDX60 would

dsRNA. After 24 h, cell lysates were prepared and luciferase activity was measured. (E and F) siRNA for DDX60 or control siRNA was transfected into HEK293 cells. The cells were left unstimulated or stimulated with poly(I · C), and expression of IFN-β and DDX60 mRNA was measured by RT-qPCR. Expression values were normalized using GAPDH. (G) siRNA for DDX60 or the control was transfected into HEK293 cells together with DDX60-expressing vector. The DDX60 protein was observed by Western blotting. (H) Vectors expressing TICAM-1 and/or DDX60 were transfected into HEK293 cells together with the p125luc reporter and *Renilla* luciferase plasmids. After 24 h, the cell lysates were prepared and luciferase activities were measured. (I) Vectors expressing TLR3 and/or DDX60 were transfected into HEK293 cells together with the p125luc reporter and *Renilla* luciferase plasmids. After 24 h, the cells were left unstimulated or stimulated with poly(I · C) for 4 h, the cell lysates were prepared, and luciferase activity was measured. (J and K) HeLa cells expressing shRNA for DDX60 (J) or EXOSC4 (K) were stimulated with 50 μg/ml of poly(I · C) (no transfection) (J) or dsRNA (transfection) (K). RT-qPCR was performed to measure IFN-β mRNA expression. (L) HeLa cells expressing shRNA for GFP, EXOSC4, or EXOSC5 were infected with VSV at an MOI of 1. Levels of induction of IFN-β mRNA were calculated as described for panel J. (M and N) Empty or IPS-1-expressing vector (M) and RIG-I CARD-, MDA5-, or TBK1-expressing vector (N) were transfected into control or DDX60 knockdown HEK293 cells together with p125luc reporter and *Renilla* luciferase plasmids. After 24 h, cell lysates were prepared and luciferase activity was measured. (O) shRNA for DDX60 did not inhibit the signaling from TLR3 (H to J). Although DDX60 promotes RLR-dependent signaling (A to E), shRNA for DDX60 did not reduce the signaling induced by RIG-I CARD, MDA5, IPS-1, or TBK1 overexpression (M and N). These data suggest that shRNA suppresses signaling upstream of RIG-I and MDA5.

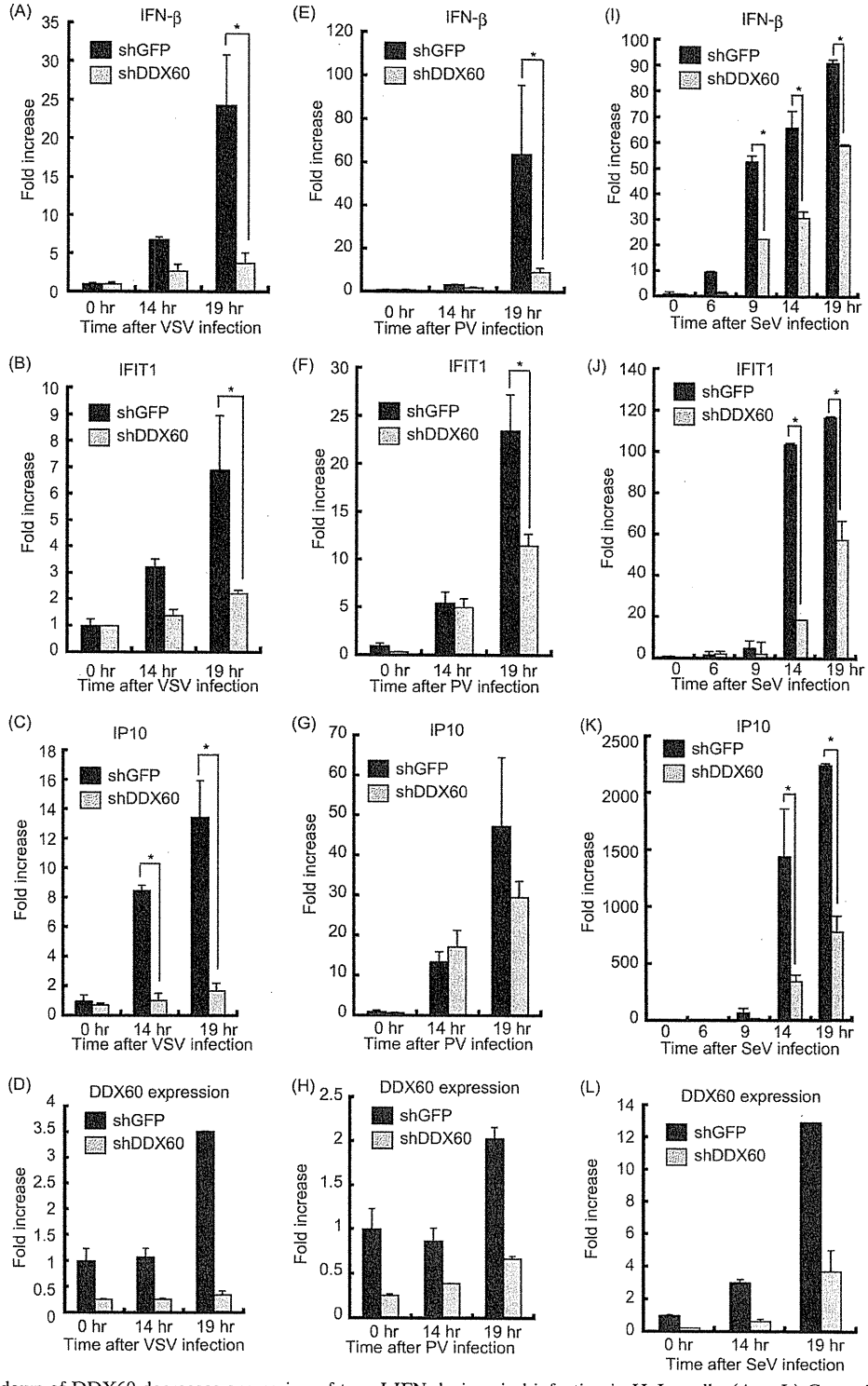

FIG. 11. Knockdown of DDX60 decreases expression of type I IFN during viral infection in HeLa cells. (A to L) Control cells or HeLa cells from a stable cell line expressing shRNA for DDX60 were infected with VSV (A to D), PV (E to H), or SeV (I to L). Total RNA was extracted at the indicated times. RT-qPCR was performed to measure expression of IFN-β (A, E, and I), IFIT1 (B, F, and J), IP10 (C, G, and K), and DDX60 (D, H, and L). The expression level of each sample was normalized to GAPDH expression.

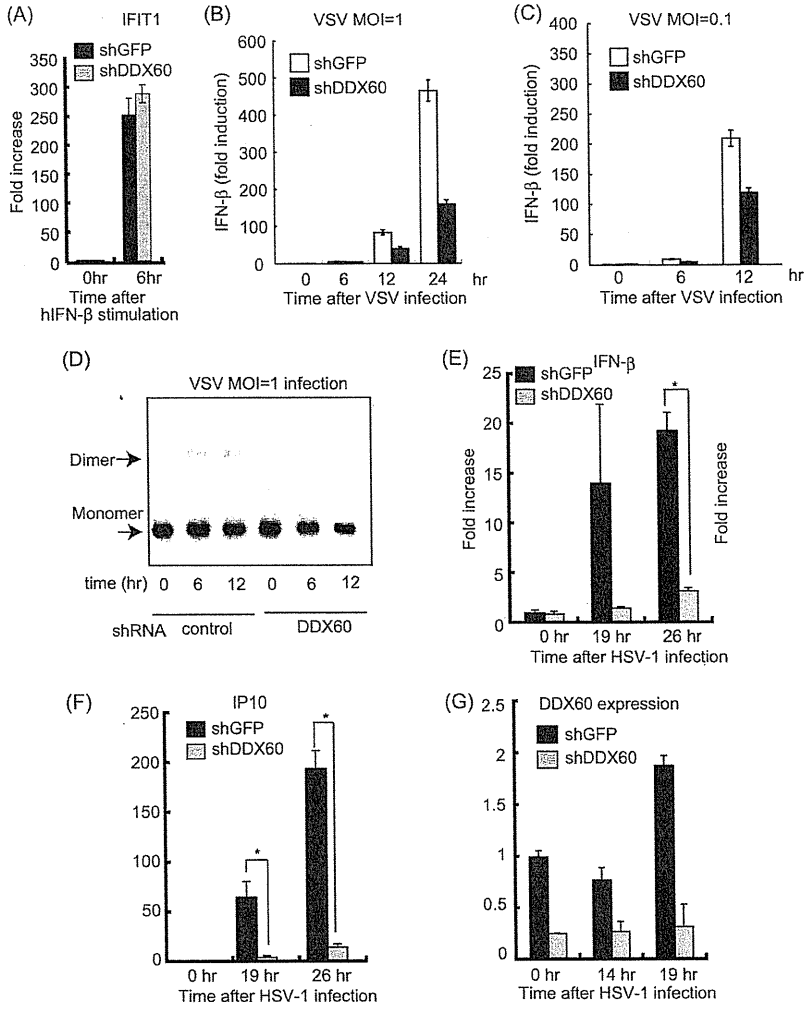

FIG. 12. Effects of DDX60 knockdown on antiviral responses. (A to C) Control or DDX60 knockdown cells were stimulated with human IFN-β (A) or infected with VSV at an MOI of 1 (B) or 0.1 (C), and expression of IFIT1 (A) and IFN-β (B and C) mRNA was examined by RT-qPCR. (D) Control or DDX60 knockdown HEK293 cells were infected with VSV at an MOI of 1, and cell lysates were prepared at the indicated times. Lysates were analyzed by native PAGE, and Western blot analysis was performed with anti-IRF-3 antibody. (E to G) Control or DDX60 knockdown HeLa cells were infected with HSV-1, and total RNA was extracted at the indicated times. RT-qPCR was performed to examine expression of IFN-β (E), IP10 (F), and DDX60 (G).

bind to viral RNA. The gel shift assay showed that DDX60 helicase can bind to dsRNA, and the pulldown assay showed that coexpression of DDX60 with RIG-I increased the binding of RIG-I to dsRNA. Thus, we speculate that DDX60 binds to viral dsRNA and associates with RLRs during viral infection. Further study is required to reveal the precise molecular mechanism by which DDX60 activates the RLR-dependent pathway.

The DDX60 helicase domain binds to dsDNA *in vitro*, and DDX60 was required for type I IFN expression during infection with HSV-1, a DNA virus. In human cells, RIG-I is involved in the pathway activated by cytoplasmic B-DNA or DNA virus infection (1, 6, 7). AT-rich dsDNA is transcribed by RNA polymerase III, and these transcripts are recognized by RIG-I (1, 6). In contrast, Choi et al. reported that the RIG-I protein associates with B-DNA and activates the signaling (7). Previously, Takahasi et al. reported that purified RIG-I protein does not itself bind to dsDNA (46). Therefore, RIG-I seems to associate with B-DNA via another protein that directly binds to dsDNA. HSV-1 was reported to produce considerable amounts of dsRNA and to activate RIG-I and MDA5 (25, 34, 52). Thus, we do not exclude the possibility that DDX60 is involved in recognition not of dsDNA but of dsRNA derived from HSV-1. Although RIG-I and MDA5 are involved in the signaling induced by cytoplasmic B-DNA, IPS-1 is dispensable for the signaling (23). Further study is required to reveal the molecular mechanism by which DDX60 plays an important role in the signaling induced by cytoplasmic B-DNA.

In addition to the *DDX60* gene, the human genome includes the closely related *DDX60L* gene, which is located 5′ upstream of *DDX60* on chromosome IV. However, the mouse genome encodes only one DDX60 protein. Our phylogenetic analysis indicated that the mouse gene is a shared ancestor of human *DDX60* and *DDX60L* genes, and a pilot study has revealed that

DDX60L is expressed after viral infection (unpublished results). Therefore, DDX60L is also expected to be an antiviral protein. Considering that knockdown of DDX60 severely reduced type I IFN expression after viral infection, there seem to be functional differences between DDX60 and 60L. Further study is required to reveal the functional differences between DDX60 and 60L.

The amino acid sequence of DDX60 is weakly similar to those of the exosome cofactors SKIV2L and SKIV2L2. In immunoprecipitation experiments, DDX60 protein was found to coimmunoprecipitate with core components of the RNA exosome. However, we could not determine the physiological role of the interaction between DDX60 and RNA exosome by knockdown analysis. We examined whether or not knockdown of DDX60 and the RNA exosome delays degradation of viral genomic RNA. We found that knockdown of DDX60 or RNA exosome components does not substantially delay degradation of transfected viral RNA (unpublished results). This observation is consistent with our results showing that knockdown of the RNA exosome does not increase viral titers. However, we do not exclude the possibility that the RNA exosome is involved in antiviral responses. There exist several antiviral nucleases, such as RNase L and ISG20. Thus, it is possible that those antiviral nucleases compensate for the defect of the RNA exosome. This possibility is not surprising, because there are several redundant pathways in the innate immune system. For example, poly(I · C) is a ligand common to TLR3 and MDA5; thus, not single but double knockout is required to abolish poly(I · C)-dependent NK cell cytotoxicity (27). Type I IFNs are produced from various kinds of cells, such as fibroblasts, dendritic cells, and macrophages; thus, we do not exclude the possibility that the RNA exosome performs some roles in DDX60 antiviral activity in other cells. The RNA exosome is required to maintain the integrity of host RNA and to disrupt RNA that lacks a 5′ catabolite gene activator protein (CAP) or 3′ poly(A) tail. Thus, it is also possible that DDX60 is involved in host RNA integrity. Further study is required to reveal the physiological role of the association of DDX60 with the RNA exosome.

In single-cell organisms such as budding yeast (*S. cerevisiae*), Ski2 plays a major role in the antiviral response to dsRNA virus. DDX60, a homolog of Ski2, is conserved among eukaryotes. For example, DDX60 is also encoded by the *Caenorhabditis elegans* genome. In a pilot study, we found nematode DDX60 expression to be increased after viral infection (unpublished results), leading us to predict that DDX60 possesses antiviral activity in this species as well. Phylogenetic tree analysis has shown that antiviral helicases such as DDX60, RLRs, and Dicer are clustered into one node. Considering that budding yeast uses Ski2 helicase for its antiviral activity, Ski2-DDX60 protein might represent the most primitive antiviral helicase, which has since diverged into several distinct but similar proteins, such as Dicer and RLRs.

ACKNOWLEDGMENTS

This work was supported in part by grants-in-aid from the Ministry of Education, Science and Culture of Japan, the Ministry of Health, Labor, and Welfare of Japan, Mitsubushi Foundation, and Akiyama Foundation.

We thank K. Matsumoto, H. Saito (National Research Institute for Child Health and Development), and H. Takaki for microarray data.

REFERENCES

1. **Ablasser, A., et al.** 2009. RIG-I-dependent sensing of poly(dA:dT) through the induction of an RNA polymerase III-transcribed RNA intermediate. Nat. Immunol. **10:**1065–1072.
2. **Akazawa, T., et al.** 2007. Antitumor NK activation induced by the Toll-like receptor 3-TICAM-1 (TRIF) pathway in myeloid dendritic cells. Proc. Natl. Acad. Sci. U. S. A. **104:**252–257.
3. **Barral, P. M., et al.** 2007. MDA-5 is cleaved in poliovirus-infected cells. J. Virol. **81:**3677–3684.
4. **Brouwer, R., et al.** 2001. Three novel components of the human exosome. J. Biol. Chem. **276:**6177–6184.
5. **Chen, G., X. Guo, F. Lv, Y. Xu, and G. Gao.** 2008. p72 DEAD box RNA helicase is required for optimal function of the zinc-finger antiviral protein. Proc. Natl. Acad. Sci. U. S. A. **105:**4352–4357.
6. **Chiu, Y. H., J. B. Macmillan, and Z. J. Chen.** 2009. RNA polymerase III detects cytosolic DNA and induces type I interferons through the RIG-I pathway. Cell **138:**576–591.
7. **Choi, M. K., et al.** 2009. A selective contribution of the RIG-I-like receptor pathway to type I interferon responses activated by cytosolic DNA. Proc. Natl. Acad. Sci. U. S. A. **106:**17870–17875.
8. **Cui, S., et al.** 2008. The C-terminal regulatory domain is the RNA 5′-triphosphate sensor of RIG-I. Mol. Cell **29:**169–179.
9. **Dangel, A. W., L. Shen, A. R. Mendoza, L. C. Wu, and C. Y. Yu.** 1995. Human helicase gene SKI2W in the HLA class III region exhibits striking structural similarities to the yeast antiviral gene SKI2 and to the human gene KIAA0052: emergence of a new gene family. Nucleic Acids Res. **23:**2120–2126.
10. **Ebihara, T., et al.** 2010. Identification of a polyI:C-inducible membrane protein that participates in dendritic cell-mediated natural killer cell activation. J. Exp. Med. **207:**2675–2687.
11. **Gack, M. U., et al.** 2007. TRIM25 RING-finger E3 ubiquitin ligase is essential for RIG-I-mediated antiviral activity. Nature **446:**916–920.
12. **Galiana-Arnoux, D., C. Dostert, A. Schneemann, J. A. Hoffmann, and J. L. Imler.** 2006. Essential function in vivo for Dicer-2 in host defense against RNA viruses in drosophila. Nat. Immunol. **7:**590–597.
13. **Gao, D., et al.** 2009. REUL is a novel E3 ubiquitin ligase and stimulator of retinoic-acid-inducible gene-I. PLoS One **4:**e5760.
14. **Guo, X., J. Ma, J. Sun, and G. Gao.** 2007. The zinc-finger antiviral protein recruits the RNA processing exosome to degrade the target mRNA. Proc. Natl. Acad. Sci. U. S. A. **104:**151–156.
15. **Hayakawa, S., et al.** 2011. ZAPS is a potent stimulator of signaling mediated by the RNA helicase RIG-I during antiviral responses. Nat. Immunol. **12:**37–44.
16. **Hornung, V., et al.** 2006. 5′-Triphosphate RNA is the ligand for RIG-I. Science **314:**994–997.
17. **Houseley, J., J. LaCava, and D. Tollervey.** 2006. RNA-quality control by the exosome. Nat. Rev. Mol. Cell Biol. **7:**529–539.
18. **Houseley, J., and D. Tollervey.** 2009. The many pathways of RNA degradation. Cell **136:**763–776.
19. **Kato, H., et al.** 2005. Cell type-specific involvement of RIG-I in antiviral response. Immunity **23:**19–28.
20. **Kato, H., et al.** 2008. Length-dependent recognition of double-stranded ribonucleic acids by retinoic acid-inducible gene-I and melanoma differentiation-associated gene 5. J. Exp. Med. **205:**1601–1610.
21. **Kato, H., et al.** 2006. Differential roles of MDA5 and RIG-I helicases in the recognition of RNA viruses. Nature **441:**101–105.
22. **Kawai, T., et al.** 2005. IPS-1, an adaptor triggering RIG-I- and Mda5-mediated type I interferon induction. Nat. Immunol. **6:**981–988.
23. **Kumar, H., et al.** 2006. Essential role of IPS-1 in innate immune responses against RNA viruses. J. Exp. Med. **203:**1795–1803.
24. **Li, X., et al.** 2009. The RIG-I-like receptor LGP2 recognizes the termini of double-stranded RNA. J. Biol. Chem. **284:**13881–13891.
25. **Melchjorsen, J., et al.** 2010. Early innate recognition of herpes simplex virus in human primary macrophages is mediated via the MDA5/MAVS-dependent and MDA5/MAVS/RNA polymerase III-independent pathways. J. Virol. **84:**11350–11358.
26. **Meylan, E., et al.** 2005. Cardif is an adaptor protein in the RIG-I antiviral pathway and is targeted by hepatitis C virus. Nature **437:**1167–1172.
27. **Miyake, T., et al.** 2009. Poly I:C-induced activation of NK cells by CD8 alpha+ dendritic cells via the IPS-1 and TRIF-dependent pathways. J. Immunol. **183:**2522–2528.
28. **Oshiumi, H., et al.** 2010. Hepatitis C virus core protein abrogates the DDX3 function that enhances IPS-1-mediated IFN-beta induction. PLoS One **5:**e14258.
29. **Oshiumi, H., M. Matsumoto, K. Funami, T. Akazawa, and T. Seya.** 2003. TICAM-1, an adaptor molecule that participates in Toll-like receptor 3-mediated interferon-beta induction. Nat. Immunol. **4:**161–167.
30. **Oshiumi, H., M. Matsumoto, S. Hatakeyama, and T. Seya.** 2009. Riplet/RNF135, a RING finger protein, ubiquitinates RIG-I to promote interferon-beta induction during the early phase of viral infection. J. Biol. Chem. **284:**807–817.

31. **Oshiumi, H., et al.** 2010. The ubiquitin ligase Riplet is essential for RIG-I-dependent innate immune responses to RNA virus infection. Cell Host Microbe **8:**496–509.
32. **Oshiumi, H., K. Sakai, M. Matsumoto, and T. Seya.** 1 February 2010, posting date. DEAD/H BOX 3 (DDX3) helicase binds the RIG-I adaptor IPS-1 to up-regulate IFN-beta inducing potential. Eur. J. Immunol. doi:10.1002/eji.200940203.
33. **Pippig, D. A., et al.** 2009. The regulatory domain of the RIG-I family ATPase LGP2 senses double-stranded RNA. Nucleic Acids Res. **37:**2014–2025.
34. **Rasmussen, S. B., et al.** 2009. Herpes simplex virus infection is sensed by both Toll-like receptors and retinoic acid-inducible gene-like receptors, which synergize to induce type I interferon production. J. Gen. Virol. **90:**74–78.
35. **Rehwinkel, J., et al.** 2010. RIG-I detects viral genomic RNA during negative-strand RNA virus infection. Cell **140:**397–408.
36. **Saito, T., et al.** 2007. Regulation of innate antiviral defenses through a shared repressor domain in RIG-I and LGP2. Proc. Natl. Acad. Sci. U. S. A. **104:**582–587.
37. **Saito, T., D. M. Owen, F. Jiang, J. Marcotrigiano, and M. Gale, Jr.** 2008. Innate immunity induced by composition-dependent RIG-I recognition of hepatitis C virus RNA. Nature **454:**523–527.
38. **Satoh, T., et al.** 26 January 2010, posting date. LGP2 is a positive regulator of RIG-I- and MDA5-mediated antiviral responses. Proc. Natl. Acad. Sci. U. S. A. doi:10.1073/pnas.0912986107.
39. **Schlee, M., et al.** 2009. Recognition of 5′ triphosphate by RIG-I helicase requires short blunt double-stranded RNA as contained in panhandle of negative-strand virus. Immunity **31:**25–34.
40. **Schmidt, A., et al.** 2009. 5′-Triphosphate RNA requires base-paired structures to activate antiviral signaling via RIG-I. Proc. Natl. Acad. Sci. U. S. A. **106:**12067–12072.
41. **Schröder, M., M. Baran, and A. G. Bowie.** 2008. Viral targeting of DEAD box protein 3 reveals its role in TBK1/IKKepsilon-mediated IRF activation. EMBO J. **27:**2147–2157.
42. **Seth, R. B., L. Sun, C. K. Ea, and Z. J. Chen.** 2005. Identification and characterization of MAVS, a mitochondrial antiviral signaling protein that activates NF-kappaB and IRF 3. Cell **122:**669–682.
43. **Soulat, D., et al.** 2008. The DEAD-box helicase DDX3X is a critical component of the TANK-binding kinase 1-dependent innate immune response. EMBO J. **27:**2135–2146.
44. **Sun, Q., et al.** 2006. The specific and essential role of MAVS in antiviral innate immune responses. Immunity **24:**633–642.
45. **Takahasi, K., et al.** 2009. Solution structures of cytosolic RNA sensor MDA5 and LGP2 C-terminal domains: identification of the RNA recognition loop in RIG-I-like receptors. J. Biol. Chem. **284:**17465–17474.
46. **Takahasi, K., et al.** 2008. Nonself RNA-sensing mechanism of RIG-I helicase and activation of antiviral immune responses. Mol. Cell **29:**428–440.
47. **van Dijk, E. L., G. Schilders, and G. J. Pruijn.** 2007. Human cell growth requires a functional cytoplasmic exosome, which is involved in various mRNA decay pathways. RNA **13:**1027–1035.
48. **van Rij, R. P., et al.** 2006. The RNA silencing endonuclease Argonaute 2 mediates specific antiviral immunity in Drosophila melanogaster. Genes Dev. **20:**2985–2995.
49. **Venkataraman, T., et al.** 2007. Loss of DExD/H box RNA helicase LGP2 manifests disparate antiviral responses. J. Immunol. **178:**6444–6455.
50. **Walker, J. E., M. Saraste, M. J. Runswick, and N. J. Gay.** 1982. Distantly related sequences in the alpha- and beta-subunits of ATP synthase, myosin, kinases and other ATP-requiring enzymes and a common nucleotide binding fold. EMBO J. **1:**945–951.
51. **Wang, X. H., et al.** 2006. RNA interference directs innate immunity against viruses in adult Drosophila. Science **312:**452–454.
52. **Weber, F., V. Wagner, S. B. Rasmussen, R. Hartmann, and S. R. Paludan.** 2006. Double-stranded RNA is produced by positive-strand RNA viruses and DNA viruses but not in detectable amounts by negative-strand RNA viruses. J. Virol. **80:**5059–5064.
53. **Wickner, R. B.** 1996. Double-stranded RNA viruses of Saccharomyces cerevisiae. Microbiol. Rev. **60:**250–265.
54. **Widner, W. R., and R. B. Wickner.** 1993. Evidence that the SKI antiviral system of Saccharomyces cerevisiae acts by blocking expression of viral mRNA. Mol. Cell. Biol. **13:**4331–4341.
55. **Xu, L. G., et al.** 2005. VISA is an adapter protein required for virus-triggered IFN-beta signaling. Mol. Cell **19:**727–740.
56. **Yanai, H., et al.** 2009. HMGB proteins function as universal sentinels for nucleic-acid-mediated innate immune responses. Nature **462:**99–103.
57. **Yoneyama, M., and T. Fujita.** 2007. RIG-I family RNA helicases: cytoplasmic sensor for antiviral innate immunity. Cytokine Growth Factor Rev. **18:**545–551.
58. **Yoneyama, M., et al.** 2005. Shared and unique functions of the DExD/H-box helicases RIG-I, MDA5, and LGP2 in antiviral innate immunity. J. Immunol. **175:**2851–2858.
59. **Yoneyama, M., et al.** 2004. The RNA helicase RIG-I has an essential function in double-stranded RNA-induced innate antiviral responses. Nat. Immunol. **5:**730–737.

OPEN ACCESS Freely available online

PLoS one

Development of Mouse Hepatocyte Lines Permissive for Hepatitis C Virus (HCV)

Hussein Hassan Aly[1], Hiroyuki Oshiumi[1], Hiroaki Shime[1], Misako Matsumoto[1], Taka Wakita[2], Kunitada Shimotohno[3], Tsukasa Seya[1]*

1 Department of Microbiology and Immunology, Hokkaido University Graduate School of Medicine, Sapporo, Hokkaido, Japan, **2** Department of Virology II, National Institute of Infectious Diseases, Shinjuku, Tokyo, Japan, **3** Research Institute, Chiba Institute of Technology, Narashino, Chiba, Japan

Abstract

The lack of a suitable small animal model for the analysis of hepatitis C virus (HCV) infection has hampered elucidation of the HCV life cycle and the development of both protective and therapeutic strategies against HCV infection. Human and mouse harbor a comparable system for antiviral type I interferon (IFN) induction and amplification, which regulates viral infection and replication. Using hepatocytes from knockout (ko) mice, we determined the critical step of the IFN-inducing/amplification pathways regulating HCV replication in mouse. The results infer that interferon-beta promoter stimulator (IPS-1) or interferon A receptor (IFNAR) were a crucial barrier to HCV replication in mouse hepatocytes. Although both IFNARko and IPS-1ko hepatocytes showed a reduced induction of type I interferons in response to viral infection, only IPS-1-/- cells circumvented cell death from HCV cytopathic effect and significantly improved J6JFH1 replication, suggesting IPS-1 to be a key player regulating HCV replication in mouse hepatocytes. We then established mouse hepatocyte lines lacking IPS-1 or IFNAR through immortalization with SV40T antigen. Expression of human (h)CD81 on these hepatocyte lines rendered both lines HCVcc-permissive. We also found that the chimeric J6JFH1 construct, having the structure region from J6 isolate enhanced HCV replication in mouse hepatocytes rather than the full length original JFH1 construct, a new finding that suggests the possible role of the HCV structural region in HCV replication. This is the first report on the entry and replication of HCV infectious particles in mouse hepatocytes. These mouse hepatocyte lines will facilitate establishing a mouse HCV infection model with multifarious applications.

Citation: Aly HH, Oshiumi H, Shime H, Matsumoto M, Wakita T, et al. (2011) Development of Mouse Hepatocyte Lines Permissive for Hepatitis C Virus (HCV). PLoS ONE 6(6): e21284. doi:10.1371/journal.pone.0021284

Editor: Jacques Zimmer, Centre de Recherche Public de la Santé (CRP-Santé), Luxembourg

Received May 13, 2011; **Accepted** May 24, 2011; **Published** June 22, 2011

Funding: This work was supported in part by Grants-in-Aid from the Ministry of Education, Science, and Culture (Specified Project for Advanced Research), the Ministry of Health, Labor, and Welfare of Japan, and the Hokkaido University Leader Development System in the Basic Interdisciplinary Research Areas (L station). Supports from Mitsubishi Foundation, Mochida Foundation, NorthTec Foundation Waxman Foundation and Yakult Foundation are gratefully acknowledged. The funders had no role in study design, data collection and analysis, decision to publish, or preparation of the manuscript.

Competing Interests: The authors have declared that no competing interests exist.

* E-mail: seya-tu@pop.med.hokudai.ac.jp

Introduction

Chronic hepatitis C virus (HCV) infection is a major cause of mortality and morbidity throughout the world infecting around 3.1% of the world's population [1]. The development of much needed specific antiviral therapies and an effective vaccine has been hampered by the lack of a suitable small animal model. The determinants restricting HCV tropism to human and chimpanzee hosts are unknown. Replication of HCV strain JFH1 has been demonstrated in mouse cells only upon antibody selection [2], highlighting the very limited replication efficiency. Human CD81 and occludin have been implicated as important entry receptors for retrovirus particles bearing HCV glycoproteins, HCV pseudoparticles (HCVpp), into NIH3T3 murine cells [3]. However, HCV infection, spontaneous replication and particle production by mouse cells have not yet been reported.

In mammalian cells, the host detects and responds to infection by RNA-viruses, including HCV, by primarily recognizing viral RNA through several distinct pathogen recognition receptors (PRRs), including the cell surface and endosomal RNA sensors Toll-like receptors 3 and 7 (TLR3 and TLR7), and the cytoplasmic RNA sensors retinoic acid-inducible gene I (RIG-I) and melanoma differentiation associated gene 5 (MDA5) [4]. The detection of virus infection by these receptors leads to the induction of interferons (IFNs) and their downstream IFN-inducible anti-viral genes through distinct signaling pathways [5]. Type I IFN is an important regulator of viral infections in the innate immune system [6]. Another type of IFN, IFN-lambda, affects the prognosis of HCV infection, and its response to antiviral therapy [7,8].

Mutations impairing the function of the RIG-I gene and the induction of IFN were essential in establishing HCV infectivity in human HuH7.5 cells [9]. Similarly, the HCV-NS3/4a protease is known to cleave IPS-1 adaptor molecule, inducing further downstream blocking of the IFN-inducing signaling pathway [10]. These data clearly demonstrate that the host RIG-I pathway is crucial for suppressing HCV proliferation in human hepatocytes. Using a similar strategy, we investigated whether suppressing the antiviral host innate immune system conferred any advantage on HCV proliferation in mouse hepatocytes. We examined the possibility of HCV replication in mice lacking the expression of key factors that modulate the type I IFN-inducing pathways. Only gene silencing of the IFN receptor (IFNAR) or IPS-1 was sufficient to establish spontaneous HCV replication in

mouse hepatocytes. To establish a cell line permissive for HCV replication, which is required for further *in vitro* studies of the HCV life cycle in mouse hepatocytes, we immortalized IFNAR- and IPS-1-knockout (ko) mice hepatocytes with SV40 T antigen. Upon expression of the human (h)CD81 gene, these newly established cell lines were able to support HCV infection for the first time in mouse hepatocytes. Viral factors required for HCV replication in mouse hepatocytes were also analyzed.

Results

IPS-1-mediated IFN signaling is important for HCV replication in mouse hepatocytes

As a first step in establishing HCV infection in mice, we tested the susceptibility of mouse hepatocytes to persistent expression of HCV proteins after RNA transfection. *In vitro* transcribed chimeric J6JFH1 RNA, in which the HCV structural and non-structural regions were from J6 and JFH1 isolates respectively, was transfected into hepatocytes from wild-type mice. We used a highly sensitive polyclonal antibody derived from HCV-patient serum for the detection of HCV proteins. No HCV proteins were detected five days after transfection (Fig. 1 A), suggesting that wild-type mouse hepatocytes were unable to maintain HCV replication. We then tried to find and block the pathway used by mouse hepatocytes for the detection of viral-RNA and the induction of IFN response. Mouse hepatocytes did not show the expression of either TLR3 or TLR7 as detected by RT-PCR, unlike IPS-1 and RIG-I which was fairly detected (Fig. S1), suggesting that the cytoplasmic RIG-I/IPS-1 pathway is the main pathway utilized by mouse hepatocytes for the detection of RNA viruses. We then checked the susceptibility of hepatocytes from TICAM-1ko, IPS-1ko and IFNARko mice to the prolonged expression of HCV proteins (Fig. 1B–D). Only IPS-1- and IFNARko mouse hepatocytes showed expression of J6JFH1 proteins five days after transfection (Fig. 1), indicating the importance of impaired IPS-1 and/or IFNAR receptors for HCV persistence. Similarly, the detection of the J6JFH1-RNA in transfected hepatocyte lines from various knockout mice showed higher levels in IPS-1 or IFNAR knockout cells compared to TICAM-1knockout cells in which a rapid decline of J6JFH1-RNA levels was noticed similar to the non-replicating control JFH1GND construct (Fig. S2). These data clearly suggest that the RIG-I/IPS-1 but not TLR3/TICAM-1 is the main pathway utilized for the detection of HCV-RNA and the induction of anti-viral immune response in mouse hepatocytes. Its suppression significantly improves HCV replication in mouse hepatocytes.

Establishment and characterization of immortalized mouse hepatocyte cell lines lacking expression of the IFNAR or IPS-1 gene

We further established mouse hepatocyte lines with disrupted IFNAR or IPS-1 genes through immortalization with SV40T antigen, and used these cell lines to study factors required for the HCV life cycle. Hepatocytes were transduced with SV40T-expressing lentivirus vectors. Six weeks after transduction, hepatocytes transduced with SV40T showed continuous proliferation and clonally proliferating hepatocyte lines were selected. SV40T-immortalized IFNARko and IPS-1ko clones were designated IRK (Fig. 2 A) and IPK (Fig. 2 B), respectively. 20 IRK and 19 IPK clones were picked up, of which IRK clones 2 and 4 (IRK2 and IRK4) and IPK clones 10 and 17 (IPK10 and IPK17) were most closely related to primary mouse hepatocytes in term of differentiation (Fig. 2 C) and were used in the following experiments. Expression of SV40T was confirmed by RT-PCR analysis (data not shown). IRK2, IRK4, IPK10 and IPK17, but not the non-hepatocytic NIH3T3 cells, displayed albumin and hepatocyte nuclear factor 4 (HNF4) expression similar to that observed in liver tissue, but did not express the bile duct marker, cytokeratin. IRK and IPK cells did not show expression of IFNAR and IPS-1 respectively (Fig. 2 C).

Replication of the HCV genome in IRK and IPK cells

To assess the permissiveness of the established cell lines to HCV replication, we transduced IRK4 and IPK17 cells with J6JFH1 RNA and monitored the HCV protein and RNA levels by IF (Fig. 3 A) and real time RT-PCR (Fig. 3 B). The number of cells expressing HCV proteins, as detected by IF, increased over time, indicating the continuous proliferation of J6JFH1 in these cells. However, the ratio between infected and non-infected cells did not significantly change over time for 7 days after transfection. Similarly, the amount of total J6JFH1 RNA in 1 μg of total cellular RNA was reasonably constant. By contrast, the level of

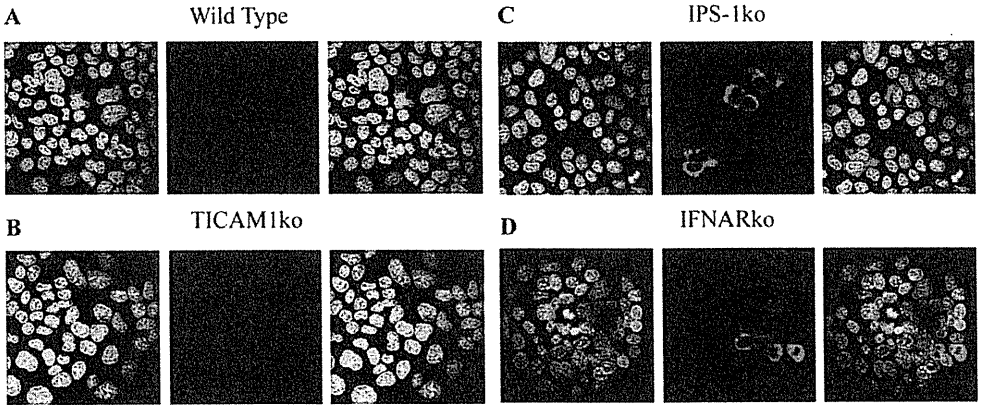

Figure 1. IF detection of of J6JFH1 proteins' expression 5 days after transfection of J6JFH1-RNA through electroporation into wild type (A), TICAM-1ko (B), IPS-1ko (C), and IFNARko (D), freshly isolated primary hepatocytes. A highly sensitive polyclonal antibody extracted from HCV-patient serum (AbS3) was used for the detection. Staining of the uninfected hepatocytes from different Ko mice was also performed and they showed negative for HCV proteins (data not shown).
doi:10.1371/journal.pone.0021284.g001

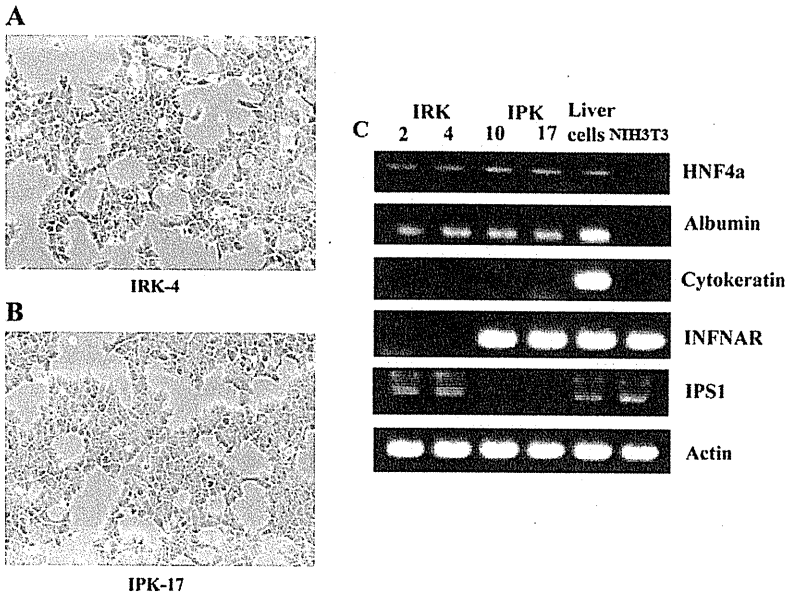

Figure 2. Morphological characteristics of IRK-4 (A) and IPK-17 (B) cells. (C) RT analysis for the expression of albumin, HNF4, cytokeratin, interferon A receptor, and IPS-1 in 2 IFNAR-KO cell lines (IRK2 and 4), 2 IPS-1-KO cell lines (IPK-10 and 17), total liver, and NIH3T3 cells.
doi:10.1371/journal.pone.0021284.g002

JFH1GND RNA carrying a mutation in NS5B hampering HCV replication, rapidly declined, indicating the requirement of continuous HCV replication for the maintenance of HCV positivity in the transfected mouse hepatocytes. Similar data were obtained from IRK2 and IPK10 cells (data not shown).

IPS-1-dependent/Interferon-independent pathway is responsible for HCV's cytopathic effect

In comparison to IPS-1ko hepatocytes, J6JFH1-RNA in IFNARko were lower and decreased further after its transfection, while higher stable levels of J6JFH1-RNA were maintained in IPS-1ko cells (Fig. 3 B and Fig. S2). Similarly, larger numbers of HCV-positive cells were detected in IPS-1ko hepatocytes compared with their IFNARko counterparts (Fig. 3 A), suggesting that the IPS-1 disruption benefits HCV replication in a distinct manner from IFNAR disruption. To measure the interferon induction after RNA virus infection in those cells, we used a highly infectious RNA-Virus (VSV) and measured the induction of interferon after its infection. All the interferons measured showed similar suppression of induction in IFNARko and IPS-1ko hepatocytes (Fig. 4). Surprisingly, cellular cytopathic effect that was monitored after transfection of J6JFH1-RNA was markedly reduced in IPS-1ko but not in IFNARko hepatocytes after transfection (Fig. 5A). This suppression was accompanied by an increase of J6JFH1-RNA levels in IPS-1ko cells, suggesting that minimal cellular damage induced by HCV replication in IPS-1-/- cells led to the improvement of HCV proliferation in mouse hepatocytes (Fig. 5B).Reduction of HCV-induced cellular cytotoxicity (Fig.5C), and improvement of HCV replication (Fig.5D) in wild type, and IFNAR-KO cells were found when we cultured the cells with a pan-caspase inhibitor, zVAD-fmk, 2 days before and after HCV-RNA transfection. We reasoned that the IPS-1 pathway rather than the IFNAR pathway capacitates hepatocytes to induce HCV-derived apoptotic cell death and its disruption resulted in the circumvention of cell death.

Human CD81 is required for HCV infection of mouse hepatocytes

Similar to the primary mouse hepatocytes, immortalized mouse hepatocytes showed the expression of all the mouse counterparts of human HCV entry receptors (Fig. S3). Human CD81 and hOccludin, but not other human HCV receptors such as SR-B1 or claudin1, have previously been reported to be essential for HCVpp entry into NIH3T3 mouse cells [3]. We then expressed hCD81 and/or hOccludin in IRK2 and IRK4 cells using lentivirus vectors. Using a MOI of 10, 95% transfection efficiency was achieved (Fig. S4) with lentivirus vector. We next tested the effect of these proteins on HCV particle (HCVcc) infection. Human CD81 alone was found to be required for J6JFH1 infection into all IRK and IPK cells tested (Fig. S5 and Fig. 6 A, and B). For the first time in mouse hepatocytes, HCV proteins were detected in nearly 1% of the cells used for infection. These data demonstrated the importance of hCD81 in establishing HCVcc infection in mouse hepatocytes.

Viral factors affecting HCV replication in mouse hepatocytes

After successfully establishing J6JFH1 infection in mouse hepatocytes, we attempted to infect these cells with other strains of HCV. Human CD81-expressing IPK17 cells were infected with full-length JFH1FL, however, no infection was detected (data not shown). This might be due to a problem in infection and/or replication. We further examined the replication efficiency of JFH1FL, the subgenomic JFH1 replicon and the J6JFH1 chimera in two different mouse hepatocyte lines and the HuH7.5.1 cell line. The persistent expression of HCV proteins was detected seven days after RNA transfection. Although HCV proteins were detected in HuH7.5.1 cells in all cases (Fig. 7 C), only J6JFH1 proteins were detected in the mouse hepatocyte lines, suggesting for the first time the importance of the J6 structural region for the replication of HCV in mouse hepatocytes (Fig. 7 A, and B).

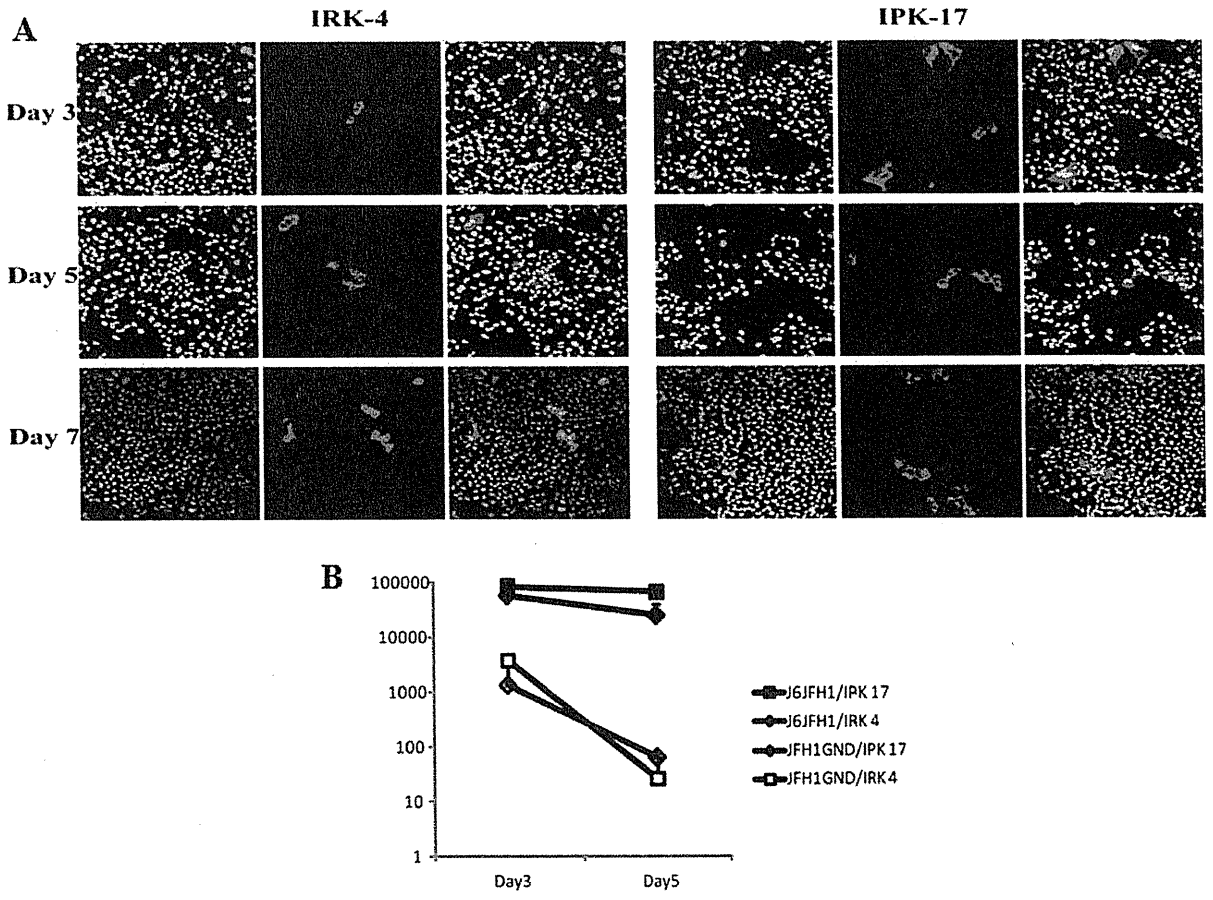

Figure 3. Proliferation of HCV in IRK4 and IPK17 cells over time as detected by immunofluorescence staining of NS5a protein using the CL1 rabbit polyclonal antibody (A) and by quantitative real-time RT-PCR analysis of HCV-RNA levels (B). JFH1GND was used as a negative control to exclude non replicating HCV-RNA. The data plotted represent the average +/− STD of 3 different experiments.
doi:10.1371/journal.pone.0021284.g003

Discussion

Gene silencing of either IPS-1 or IFNAR significantly improves HCV replication and persistence in mouse hepatocytes compared with wild-type or TICAM-1ko mice. This result demonstrated the importance of the IPS-1 pathway rather than the TICAM-1 pathway in the induction of type I IFN by HCV infection, and revealed that the IFNAR amplification pathway confers resistance to HCV in mouse hepatocytes independently of TICAM-1. In accordance with our data, HCV-NS3/4A protease is known to cleave the IPS-1 and/or RIG-I-complement molecules including DDX3 and Riplet in humans to overcome the host innate immune response, showing the importance of RIG-I/IPS-1 pathway suppression in the establishment of HCV infection [10,11,12].

To further study factors affecting the HCV life cycle in mouse hepatocytes, we established IPK and IRK immortalized mouse hepatocyte lines by transduction with SV40T antigen. The established hepatocytes cell lines showed expression of HNF4, a major hepatocyte transcription factor, required for hepatocyte differentiation and liver-specific gene expression [13]. The maintenance of hepatocellular functions was demonstrated by continuous expression of hepatocyte specific differentiation marker, albumin, and the lack of expression of the bile duct marker, cytokeratin. The close resemblance of these cell lines to primary mouse hepatocytes is crucial to ensure the physiological relevance of factors identified in these cell lines that affect the HCV life cycle.

It is worth noting that HCV replication in IPS-1ko was higher than that in IFNARko hepatocytes. Since IPS-1 is present upstream of IFNAR in the IFN-amplification pathway, this higher J6JFH1 replication efficiency in IPS-1ko hepatocytes suggested the presence of an additive factor affecting HCV replication other than the induction of IFNAR-mediated type I IFN. This enhanced replication efficiency was also not accompanied by the induction of other interferon types, but was correlated with the reduction of HCV-induced apoptosis in mouse hepatocytes. This data clearly demonstrates that IPS-1 is playing an important role in the regulation of HCV infection in mouse hepatocytes through two different pathways, the IFN-induction pathways and another new IFN-independent pathway, leading to apoptotic cell death and elimination of HCV-harboring hepatocytes. The cytopathic effect of HCV infection in human cells is still contradictory. Although, some reports showed the induction of apoptosis and cell death by HCV infection in human hepatocytes [14,15,16], others showed suppression of apoptosis by HCV proteins [17,18]. This difference may be due to the different cell lines used in the different studies. Almost all the studies reporting HCV-induced apoptosis used

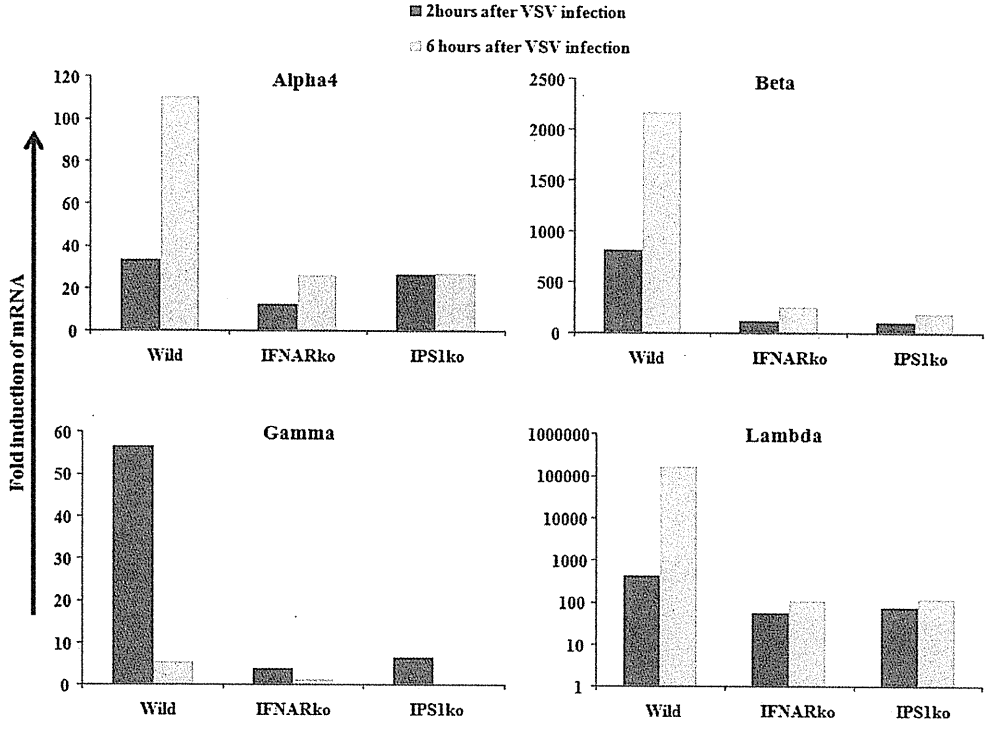

Figure 4. Wild type, IFNARko, and IPS-1ko mice hepatocytes were infected with mock or VSV virus, 2 and 6 hours later, total RNA was extracted from the cells, and interferon alpha, beta, gamma and lambda mRNA induction levels were measured by real-time RT-PCR. Similar results were obtained from 2 different experiments, each was performed in duplicates. The data plotted represent the mean duplicate readings in one of them.
doi:10.1371/journal.pone.0021284.g004

hepatocellular carcinoma cell lines. Since it has been established that the inability to undergo apoptosis is essential for the development of cancer [19,20,21], our use of immortalized, non-cancerous hepatocytes may make it possible to reproduce the physiological response of the cells to HCV infection more closely. The IPS-1 regulation of cell death following the introduction of HCV-RNA may also regulate the effector cell function. It is likely that hepatocyte debris generated secondary to intrinsic production of viral dsRNA in HCV-infected hepatocytes affect the antiviral effector response of the immune system through maturation of dendritic cells [22]. Hence, the effector cell activation may be enhanced by the induction of cell death through the IPS-1 pathway in hepatocytes which may facilitate producing dsRNA-containing debris.

In comparison to the JFH1GND construct with deficient replication that showed a rapid reduction in its RNA levels over time after transfection into mouse hepatocytes, J6JFH1 RNA was detected at four-log higher levels and was maintained at a relatively stable levels in IPS-1ko hepatocytes. Although the number of mouse cells expressing HCV proteins was found to increase over time, as detected by IF, the ratio between HCV-negative and -positive cells did not show any significant change for 7 days after transfection and increased after 10 days (data not shown). This indicates a negative selection of HCV-bearing cells over time which may be due to slower cellular replication, or loss of HCV replication. Another possibility may be that HCV infection is affected by the presence of an inhibitory factor possibly triggered by HCV replication or the lack of a human host factor required for HCV replication. Due to the initial replication of HCV in the transfected IPK and IRK mouse hepatocytes for the first 7 days and the establishment of infection, we favor the presence of a possible inhibitory factor that may be triggered by HCV replication. Another factor that also limits HCV spread in mouse hepatocytes is the failure of HCV to produce infectious particles in these cells (data no shown).

Using this newly established immortalized mouse hepatocyte line, we found that although J6JFH1, JFH1FL and the subgenomic JFH1 replicon all share a similar non-structural region derived from isolate JFH1 that is required for HCV replication, and although all of these constructs can replicate efficiently in HuH7.5.1 cells, strikingly, only J6JFH1 carrying the J6 structural region replicated in mouse hepatocytes. This indicates the importance of the J6 structural region and/or the chimeric construct between J6 and JFH1 for HCV replication in mouse hepatocytes. Structural regions are known to be important for HCV entry and/or particle formation [23], but this is the first time that their importance in replication in HCV-bearing cells has been demonstrated. This finding clearly shows the importance of non-hepatoma cell lines with less genetic abnormalities and mutations for the discovery of new aspects of the life cycle of HCV.

Although, the co-expression of human CD81 and Occludin genes was found to be important for HCVpp entry into murine NIH3T3 cells [3], the expression of hCD81 alone was sufficient for J6JFH1 entry into mouse hepatocytes. This may be explained by the different cell lines used in the different studies. In contrast to NIH3T3 cells, we used immortalized hepatocytes that showed close physiological resemblance to primary mouse hepatocytes and showed the expression of all the mouse counterparts of HCV entry

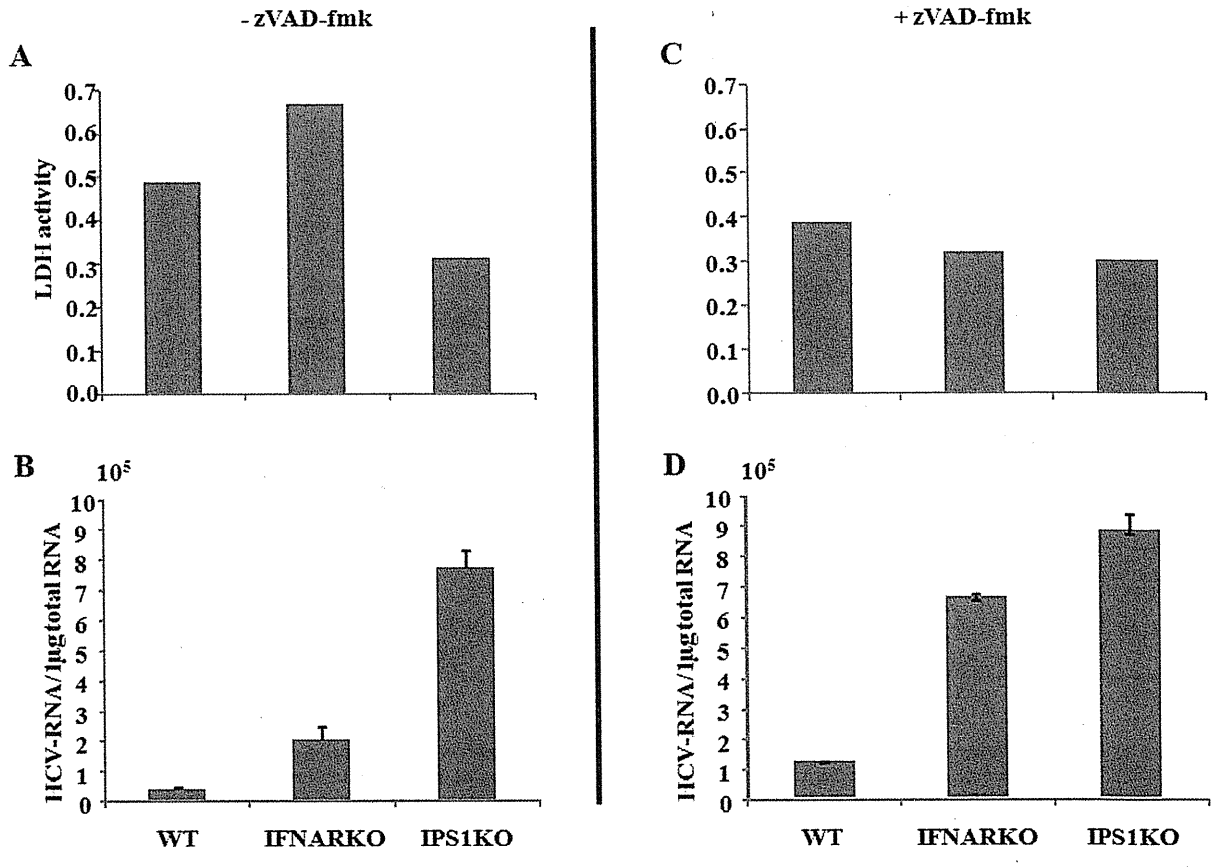

Figure 5. Measurement of J6JFH1 mediated cytopathic effect in wild type, IFNARko, and IPS-1ko mouse hepatocytes. Cultrure medium were left untreated (A;B) or treated with 20 μM of zVAD-fmK (C;D) 2 days before and after J6JFH1-RNA transfection. One day after transfection of J6JFH1-RNA, culture medium was discarded and cells were washed with PBS. A new medium was added and cells were cultured for another 24 hours. The LDH activity in the culture medium was measured in 2 different experiments in duplicates and showed similar results, the average levels of a duplicate from a single experiment was plotted (A, C). HCV-RNA titers in the cells were also measured using real-time RT-PCR (B, D), the data shown represent the mean +/− STD of 3 different experiments.
doi:10.1371/journal.pone.0021284.g005

receptors. A study from a different group showed that adaptive mutations in HCV envelope proteins allowing its interaction with murine CD81 is enough for efficient HCVpp entry without the expression of any human entry receptors in murine cells [24]. This report, together with ours, suggest that CD81 is the main human host restriction factor for HCV entry, and that overcoming this problem either by HCV adaptation to murine CD81, or the expression of human CD81 in murine hepatocytes is essential for HCV entry. Although our lentivirus transfection efficiency with CD81 was around 95% in IPK and IRK clones, only 1% of the cells were prone to infection with HCVcc. Also, HCVpp showed lower entry levels in those cells compared to HuH7.5.1 cells (Fig. S6). This suggests that hCD81 expression is the minimum and most crucial requirement for HCV entry into mouse hepatocytes. The discovery and expression of other co-receptors facilitating HCV entry in human cells is still required for efficient and robust HCV infection.

In summary, the suppression of IPS-1 is important for the establishment of HCV infection and replication in mouse hepatocytes through the suppression of both interferon induction and interferon independent J6JFH1-induced cytopathic effect. We have established hepatocytes lines from IPS-1 and IFNARko mice that support HCV replication and infection. These cell lines will be very useful in identifying other species restriction factors and viral determinants required for further establishment of a robust and efficient HCV life cycle in mouse hepatocytes. Using those cells, we showed for the first time the importance of HCV structural region for viral replication. IRF3ko mouse embryo fibroblasts (MEFs) were previously shown to support HCV replication more efficiently than wild MEFs [25]. Since the knockout of IPS-1 mainly suppresses signaling in response to virus RNA detection, and maintains an intact IFN response to other stimulants, it may result in minimum interference to adaptive immune responses as compared to IRF3 or IFNARko. Therefore, further development of hCD81-transgenic IPS-1ko mice may serve as a good model for the study of immunological responses against HCV infection. This mouse model can be used as a backbone for any further future models supporting robust HCV infectivity for the study of HCV pathogenesis, propagation and vaccine development.

Material and Methods

Cell culture

HuH7.5.1 cells were cultured in high-glucose Dulbecco's modified Eagle's medium (DMEM; Gibco/Invitrogen, Tokyo, Japan) supplemented with 2 mM L-glutamine, 100 U of penicillin/ml, 100 μg of

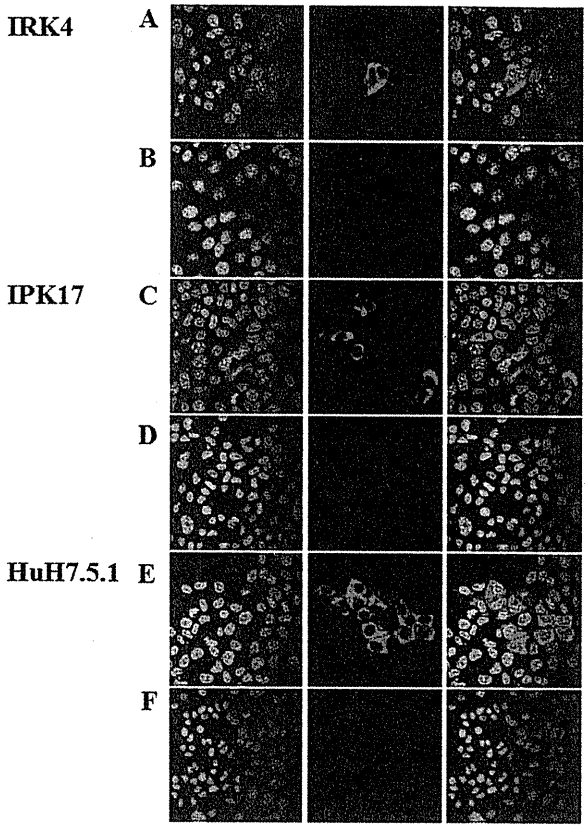

Figure 6. J6JFH1 infection into IRK-4 and IPK17 cells. HCV-NS5A protein detection in mouse IRK4 (A,B) and IPK17 (C,D) and human 7.5.1 cells (E,F). The cells were transduced with lentivirus expressing human CD81 gene at 10 MOI. 48 hours later the cells were infected with 100 times concentrated supernatant medium, collected during 1 week after transfection of HuH7.5.1 cells with J6JFH1-RNA (A, C, and E) or JFH1GND-RNA (B, D, and F).
doi:10.1371/journal.pone.0021284.g006

streptomycin/ml and 10% fetal bovine serum. Mouse primary hepatocytes were isolated from the liver using collagenase perfusion through the inferior vena cava (IVC), while clamping the animal's intrathoracic extension. Hepatocyte isolation and perfusion control were performed as previously described [26]. Primary and immortalized hepatocytes were cultured in a similar medium supplemented with: HEPES (Gibco/Invitrogen), 20 mmol/L; L-proline, 30 μg/mL; insulin (Sigma, St. Louis, MO, USA), 0.5 μg/mL; dexamethasone (Wako, Osaka, Japan), 1×10^{-7} mol/L; $NaHCO_3$, 44 mmol/L; nicotinamide (Wako), 10 mmol/L; EGF (Wako), 10 ng/mL; L-ascorbic acid 2-phosphate (Wako), 0.2 mmol/L; and MEM-non essential amino acids (Gibco/Invitrogen), 1%.

Gene-disrupted mice

All mice were backcrossed with C57BL/6 mice more than seven times before use. Toll-like receptor adaptor molecule 1 (TICAM-1) ko [27] and IPS-1ko mice [28] were generated in our laboratory (detailed information regarding the IPS-1 mice will be presented elsewhere). All mice were maintained under specific-pathogen-free conditions in the animal facility of the Hokkaido University Graduate School of Medicine (Japan).

RNA extraction, reverse transcriptase polymerase chain reaction (RT-PCR) and real-time RT-PCR

RNA was extracted from cultured cells using Trizol reagent (Invitrogen, San Diego, CA, USA) according to the manufacturer's protocol. Using 1 μg of total RNA as a template, we performed RT-PCR and real-time RT-PCR as previously described [29,30].

In vitro RNA transcription, transfection and preparation of J6JFH1 and Jfh1 viruses

In vitro RNA transcription, transfection into HuH7.5.1 or mouse hepatocytes, and preparation of J6JFH1 and JFH1 viruses, were all performed as previously reported [31]. RNA transfection into human and mouse hepatocytes was performed by electroporation using a Gene Pulser II (Bio-Rad, Berkeley, California) at 260 V and 950 Cap.

HCV infection

J6JFH1 and JFH1 concentrated medium were adjusted to contain a similar RNA copy number by real-time RT-PCR. 2×10^4 cells/well were cultured in 8-well glass chamber slides. After 24 hours, the medium was removed and replaced by concentrated medium containing JFH1 or J6JFH1 viruses. After three hours, the concentrated medium was removed, cells were washed with PBS and incubated in fresh medium for 48 hours, before the detection of infection.

Lentivirus construction, titration and infection

The gene encoding T antigen from simian virus was cloned from plasmid CSII-EF-SVT [32]. The genes encoding human CD81 and occludin were cloned from HuH-7.5.1 cells using the Zero Blunt TOPO PCR Cloning Kit (Invitrogen) according to the manufacturer's protocol. These genes were then inserted into the GFP reporter gene-containing lentiviral expression (pLBIG) vector using the *Eco*RI and *Xho*I restriction sites for SV40T and hCD81, and the *Xba*I and *Xho*I restriction sites for hOccludin. Lentivirus expression vectors were then constructed as previously described [27]. GFP expression was used for the titration of lentivirus vectors, and a multiplicity of infection (MOI) of 10 was used for the infection of mouse cells. Forty-eight hours after the transfection of hCD81 and/or hOccludin, cells were trypsinized and counted. Then, 2×10^4 cells/well were cultured in 8-well glass chamber slides for HCV infection and 5×10^4 cells/well were cultured in 12-well plates, along with 1 ml of medium containing HCVpp, for HCV entry experiments.

HCVpp construction and the detection of luciferase expression

HCVpp containing the E1 and E2 proteins from HCV isolate J6 and expressing the luciferase reporter gene were a kind gift from Dr. Thomas Pietschmann at the TWINCORE Center for Experimental and Clinical Infection Research, Germany. The production of HCVpp and the measurement of luciferase levels were performed as previously described [33].

Indirect immunofluorescence (IF)

IF expression of HCV proteins was detected in the infected cells using antibodies in the serum of chronic HCV patients or rabbit IgG anti-NS5A antibody (Cl-1) (both kind gifts from K. Shimotohno, Chiba Institute of Technology, Japan). Goat anti-human IgG Alexa 594 and goat anti-rabbit Alexa 594 (Invitrogen) were used as secondary antibodies, respectively. Fluorescence

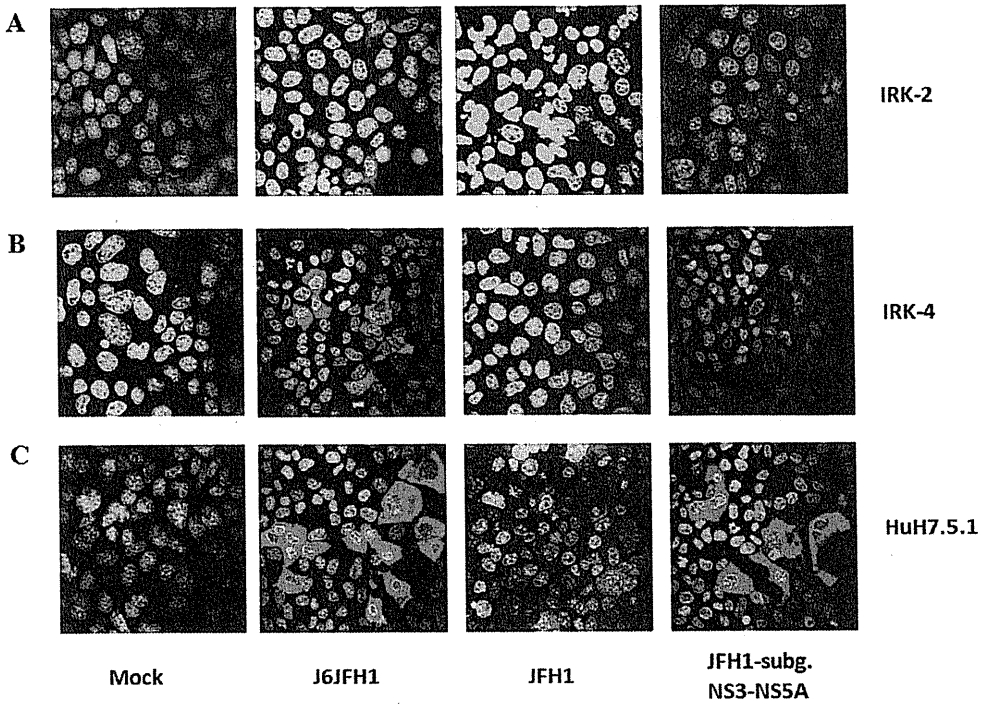

Figure 7. Detection of HCV-NS5A protein in IRK-2 (A), IRK-4 (B) and HuH-7.5 cells (C) by IF 5 days after transfection with J6JFH1, FL-JFH1 or subgenomic JFH1-RNA.
doi:10.1371/journal.pone.0021284.g007

detection was performed on a ZEISS LSM 510 Meta confocal microscope (Zeiss, Jena, Germany).

Detection of cell death

Culture medium was collected from HCV infected and control cells and used for measuring lactate dehydrogenase (LDH) levels using an LDH cytotoxicity detection kit (Takara Biomedicals, Tokyo, Japan). Light absorbance was then measured according to the manufacturer's protocol.

Ethic Statement

This study was carried out in strict accordance with the recommendations in the Guide for the Care and Use of Laboratory Animals of the National Institutes of Health. The protocol was approved by the Committee on the Ethics of Animal Experiments in the Animal Safety Center, Hokkaido University, Japan. All mice were used according to the guidelines of the institutional animal care and use committee of Hokkaido University, who approved this study as ID number: 08-0243, " Analysis of immune modulation by toll-like receptors".

Supporting Information

Figure S1 RT detection of TLR3, TLR7, RIG-I, and IPS-1 expression in mouse hepatocytes. GAPDH expression was used as internal control, and RNA from CD11c+ spleenocytes (dendritic cells) was used as positive control.
(TIF)

Figure S2 Proliferation of HCV in IPS-1, TICAM-1(TRIF) and IFNAR-knockout mouse hepatocytes over time as detected by quantitative real-time RT-PCR analysis of HCV-RNA levels. JFH1GND transfection into IPS-1 knockout cells was used as a negative control to exclude non replicating HCV RNA. The data plotted represent the average +/− STD of 3 different experiments.
(TIF)

Figure S3 RT detection of CD81, Occludin, Claudin 1, SRB1, and LDL receptor expression in primary, IRK4 and IPK17 mouse hepatocytes. GAPDH expression was used as internal control.
(TIF)

Figure S4 Estimation of the transfection efficiency of lentivirus vector expressing green fluorescent protein (GFP) as a reporter, together with hCD81 or hOccludin. 48 hours after transfection with the lentivirus vector, cells were trypsinized and GFP positive cells were detected by BD FACSCalibur (BD Biosciences).
(TIF)

Figure S5 HCV infection of IRK2 cells transfected with lentivirus expressing hCD81 and/or hOccludin. IRK2 cells were transfected with lentivirus expressing empty vector (A), hCD81 (B), hOccludin (C) or hCD81 and hOccludin (D) at a MOI of 10. After 48 hours, the cells were infected with concentrated J6JFH1 transfected 7.5.1 culture medium. After a further three hours, cells were washed with PBS and incubated in fresh medium. After another 48 hours, HCV infection was examined through the detection of HCV-NS5a protein expression by immunofluorescence staining.
(TIF)

Figure S6 HCVpp entry into mouse cells. A similar number of IPK17 and HuH7.5.1 were cultured in triplicate. IPK17 cells were only transfected with lentivirus expressing hCD81, while HuH7.5.1 cells were transfected with empty vector at a MOI of

10. After 48 hours, the medium was replaced with a new medium containing mock VSVG-pp or HCVpp expressing luciferase. After another 48 hours, pseudoparticles entry was determined by measuring the luciferase activity. In order to compare the HCVpp entry between IPK17 and HuH7.5.1 cells, the luciferase expression from VSV-Gpp entry was used an internal control, while that from HCVpp was plotted relatively.
(TIF)

Acknowledgments

We want to thank Dr. Michinori Kohara (Tokyo Metropolitan Institute for Medical Science, Tokyo, Japan); Dr. Tadatsugu Taniguchi (University of Tokyo, Yokyo, Japan); Dr. Thomas Pietschmann (Division of Experimental Virology, TWINCORE, Hannover, Germany); and Dr. Makoto Hijikata (The Institute for Virus Research, Kyoto University, Japan) for their generous supply of research material. Dr. Hussein H. Aly was supported by a JSPS postdoctoral fellowship from the Japan Society for the Promotion of Science.

Author Contributions

Conceived and designed the experiments: HHA TS. Performed the experiments: HHA HO. Analyzed the data: HHA MM HO HS TS. Contributed reagents/materials/analysis tools: KS TW. Wrote the paper: HHA.

References

1. Seto WK, Lai CL, Fung J, Hung I, Yuen J, et al. (2010) Natural history of chronic hepatitis C: Genotype 1 versus genotype 6. J Hepatol.
2. Uprichard SL, Chung J, Chisari FV, Wakita T (2006) Replication of a hepatitis C virus replicon clone in mouse cells. Virol J 3: 89.
3. Ploss A, Evans MJ, Gaysinskaya VA, Panis M, You H, et al. (2009) Human occludin is a hepatitis C virus entry factor required for infection of mouse cells. Nature 457: 882–886.
4. Diamond MS (2009) Mechanisms of evasion of the type I interferon antiviral response by flaviviruses. J Interferon Cytokine Res 29: 521–530.
5. O'Neill LA, Bowie AG (2010) Sensing and signaling in antiviral innate immunity. Curr Biol 20: R328–333.
6. Platanias LC (2005) Mechanisms of type-I- and type-II-interferon-mediated signalling. Nat Rev Immunol 5: 375–386.
7. Tanaka Y, Nishida N, Sugiyama M, Kurosaki M, Matsuura K, et al. (2009) Genome-wide association of IL28B with response to pegylated interferon-alpha and ribavirin therapy for chronic hepatitis C. Nat Genet 41: 1105–1109.
8. Thompson AJ, Muir AJ, Sulkowski MS, Ge D, Fellay J, et al. (2010) Interleukin-28B polymorphism improves viral kinetics and is the strongest pretreatment predictor of sustained virologic response in genotype 1 hepatitis C virus. Gastroenterology 139: 120–129. e118.
9. Sumpter R, Jr., Loo YM, Foy E, Li K, Yoneyama M, et al. (2005) Regulating intracellular antiviral defense and permissiveness to hepatitis C virus RNA replication through a cellular RNA helicase, RIG-I. J Virol 79: 2689–2699.
10. Foy E, Li K, Sumpter R, Jr., Loo YM, Johnson CL, et al. (2005) Control of antiviral defenses through hepatitis C virus disruption of retinoic acid-inducible gene-I signaling. Proc Natl Acad Sci U S A 102: 2986–2991.
11. Oshiumi H, Ikeda M, Matsumoto M, Watanabe A, Takeuchi O, et al. (2010) Hepatitis C virus core protein abrogates the DDX3 function that enhances IPS-1-mediated IFN-beta induction. PLoS One 5: e14258.
12. Oshiumi H, Miyashita M, Inoue N, Okabe M, Matsumoto M, et al. (2010) The ubiquitin ligase Riplet is essential for RIG-I-dependent innate immune responses to RNA virus infection. Cell Host Microbe 8: 496–509.
13. Ishiyama T, Kano J, Minami Y, Iijima T, Morishita Y, et al. (2003) Expression of HNFs and C/EBP alpha is correlated with immunocytochemical differentiation of cell lines derived from human hepatocellular carcinomas, hepatoblastomas and immortalized hepatocytes. Cancer Sci 94: 757–763.
14. Berg CP, Schlosser SF, Neukirchen DK, Papadakis C, Gregor M, et al. (2009) Hepatitis C virus core protein induces apoptosis-like caspase independent cell death. Virol J 6: 213.
15. Deng L, Adachi T, Kitayama K, Bungyoku Y, Kitazawa S, et al. (2008) Hepatitis C virus infection induces apoptosis through a Bax-triggered, mitochondrion-mediated, caspase 3-dependent pathway. J Virol 82: 10375–10385.
16. Zhu H, Dong H, Eksioglu E, Hemming A, Cao M, et al. (2007) Hepatitis C virus triggers apoptosis of a newly developed hepatoma cell line through antiviral defense system. Gastroenterology 133: 1649–1659.
17. Ray RB, Meyer K, Ray R (1996) Suppression of apoptotic cell death by hepatitis C virus core protein. Virology 226: 176–182.
18. Mankouri J, Dallas ML, Hughes ME, Griffin SD, Macdonald A, et al. (2009) Suppression of a pro-apoptotic K+ channel as a mechanism for hepatitis C virus persistence. Proc Natl Acad Sci U S A 106: 15903–15908.
19. Ladu S, Calvisi DF, Conner EA, Farina M, Factor VM, et al. (2008) E2F1 inhibits c-Myc-driven apoptosis via PIK3CA/Akt/mTOR and COX-2 in a mouse model of human liver cancer. Gastroenterology 135: 1322–1332.
20. Lowe SW, Lin AW (2000) Apoptosis in cancer. Carcinogenesis 21: 485–495.
21. Schulze-Bergkamen H, Krammer PH (2004) Apoptosis in cancer--implications for therapy. Semin Oncol 31: 90–119.
22. Ebihara T, Shingai M, Matsumoto M, Wakita T, Seya T (2008) Hepatitis C virus-infected hepatocytes extrinsically modulate dendritic cell maturation to activate T cells and natural killer cells. Hepatology 48: 48–58.
23. Mateu G, Donis RO, Wakita T, Bukh J, Grakoui A (2008) Intragenotypic JFH1 based recombinant hepatitis C virus produces high levels of infectious particles but causes increased cell death. Virology 376: 397–407.
24. Bitzegeio J, Bankwitz D, Hueging K, Haid S, Brohm C, et al. (2010) Adaptation of hepatitis C virus to mouse CD81 permits infection of mouse cells in the absence of human entry factors. PLoS Pathog 6: e1000978.
25. Lin LT, Noyce RS, Pham TN, Wilson JA, Sisson GR, et al. (2010) Replication of subgenomic hepatitis C virus replicons in mouse fibroblasts is facilitated by deletion of interferon regulatory factor 3 and expression of liver-specific microRNA 122. J Virol 84: 9170–9180.
26. Ishigami A, Fujita T, Handa S, Shirasawa T, Koseki H, et al. (2002) Senescence marker protein-30 knockout mouse liver is highly susceptible to tumor necrosis factor-alpha- and Fas-mediated apoptosis. Am J Pathol 161: 1273–1281.
27. Akazawa T, Ebihara T, Okuno M, Okuda Y, Shingai M, et al. (2007) Antitumor NK activation induced by the Toll-like receptor 3-TICAM-1 (TRIF) pathway in myeloid dendritic cells. Proc Natl Acad Sci U S A 104: 252–257.
28. Ebihara T, Azuma M, Oshiumi H, Kasamatsu J, Iwabuchi K, et al. (2010) Identification of a polyI:C-inducible membrane protein that participates in dendritic cell-mediated natural killer cell activation. J Exp Med 207: 2675–2687.
29. Aly HH, Qi Y, Atsuzawa K, Usuda N, Takada Y, et al. (2009) Strain-dependent viral dynamics and virus-cell interactions in a novel in vitro system supporting the life cycle of blood-borne hepatitis C virus. Hepatology 50: 689–696.
30. Aly HH, Shimotohno K, Hijikata M (2009) 3D cultured immortalized human hepatocytes useful to develop drugs for blood-borne HCV. Biochem Biophys Res Commun 379: 330–334.
31. Wakita T, Pietschmann T, Kato T, Date T, Miyamoto M, et al. (2005) Production of infectious hepatitis C virus in tissue culture from a cloned viral genome. Nat Med 11: 791–796.
32. Aly HH, Watashi K, Hijikata M, Kaneko H, Takada Y, et al. (2007) Serum-derived hepatitis C virus infectivity in interferon regulatory factor-7-suppressed human primary hepatocytes. J Hepatol 46: 26–36.
33. Haid S, Windisch MP, Bartenschlager R, Pietschmann T (2010) Mouse-specific residues of claudin-1 limit hepatitis C virus genotype 2a infection in a human hepatocyte cell line. J Virol 84: 964–975.

Review

Journal of Innate Immunity

J Innate Immun 2011;3:264–273
DOI: 10.1159/000326891

Received: January 20, 2011
Accepted after revision: February 24, 2011
Published online: March 29, 2011

Natural Killer Cell Activation Secondary to Innate Pattern Sensing

Tsukasa Seya Jun Kasamatsu Masahiro Azuma Hiroaki Shime
Misako Matsumoto

Department of Microbiology and Immunology, Hokkaido University Graduate School of Medicine, Sapporo, Japan

Key Words
Natural killer cell activation · Dendritic cell · Toll-like receptor 3 · TICAM-1 · MyD88

Abstract
Recent progress in understanding the outcomes of pattern-recognition by myeloid dendritic cells (mDC) allows us to delineate the pathways driving natural killer (NK) cell activation. Mouse mDC mature in response to microbial patterns and are converted to an NK cell-activating phenotype. The MyD88 pathway, the Toll/IL-1 receptor homology domain-containing adaptor molecule (TICAM)-1 (TRIF) pathway, and the interferon (IFN)-β promoter stimulator 1 (IPS-1) pathway in mDC participate in driving NK activation, as shown by analyses in knockout mice. Studies using synthetic compounds for Toll-like receptors/RIG-I-like receptors have demonstrated that mDC-NK cell contact induces NK cell activation without the participation of cytokines in mice. In vivo bone marrow transplantation analysis revealed that the IPS-1 pathway in nonmyeloid cells and the TICAM-1 pathway in mDC are crucial for dsRNA-mediated in vivo NK activation. These results infer the presence of cytokine-dependent and cytokine-independent modes of NK activation in conjunction with innate immune activation. Here, we focus on the IFN-inducing pathways and mDC-NK contact-induced NK activation and discuss the reported various NK activation modes.

Introduction

Natural killer (NK) cells have the ability to kill certain tumor cells and infected cells [1]. A number of activating and inhibitory receptors have been implicated in NK cell recognition and elimination of target cells [2]. In addition, NK cell effector functions are induced or potentiated through recognition of microbial products by innate pattern recognition receptors (PRRs) that are expressed in various cell types, including myeloid cells and NK cells. In this way, dendritic cells may induce cytokines, such as interferon (IFN)-γ, and potentiate cytotoxicity by NK cells [3]. In mice, myeloid cells stimulate NK cells through cell-cell contact and with soluble mediators [4, 5]. Many factors including cytokines and molecules supporting direct contact by immune-related cells are reported to participate in NK activation [2–5]. Myeloid dendritic cells (mDC) and macrophages (Mf) often serve as a source of such activating factors as IL-12p70, IL-18, IL-15, and type I IFN.

It is well known that type I IFN activates NK cells. However, immature mDC only subfunctionally produce type I IFN and, consequently, IFN-dependent NK activation factors are maintained at basal levels through the IFN-α receptor (IFNAR) pathway in mice [6]. Infection or inflammation stimulates additional factors that render NK activation by mDC feasible [4, 5]. Such factors that induce mDC maturation largely belong to a class of ex-

KARGER
Fax +41 61 306 12 34
E-Mail karger@karger.ch
www.karger.com

1662–811X/11/0033–0264$38.00/0

Accessible online at:
www.karger.com/jin

Dr. Tsukasa Seya
Department of Microbiology and Immunology
Graduate School of Medicine, Hokkaido University
Kita-ku, Sapporo 060-8638 (Japan)
Tel. +81 11 706 5073, E-Mail seya-tu@pop.med.hokudai.ac.jp

ogenous or endogenous pattern molecules designated pathogen-associated molecular patterns (PAMP)/damage-associated molecular patterns (DAMP) [7, 8]. Research into signaling pathways in the innate immune system has indicated that PAMP and DAMP act on PRRs in mDC/Mf and drive NK activation [4, 5, 7, 8]. In addition, membrane molecules upregulated on the surface of mDC participate in NK activation in a process known as mDC-NK contact-mediated NK activation [4, 5]. In this case, mature mDC and NK cells must be recruited to local lymph nodes, and their interactions lead to the emergence of effector NK cells in the periphery. However, it is unknown whether activation of NK cells is totally dependent on IFN or just shares the PRR pathways with IFN induction to upregulate other NK-activating molecules. Furthermore, it remains undetermined what microenvironment mDC require for maturation along with NK activation and what effectors mDC stimulate via the PRR pathways to participate in enhancing NK activity.

Recent progress in the innate pattern-sensing system suggests that mDC pattern recognition is a major event in driving mDC to an NK-activating phenotype [9–11]. These results add new insight into the currently accepted theory that the balance between a number of activating receptors and inhibitory receptors and their activation states are critical for NK activation [2, 3, 12, 13]. Insight into the mechanism behind NK cell activation may be gained via analysis of the molecular mechanisms by which PAMP/DAMP activate the immune system and, in particular, mDC. NK cells have the capacity to induce memory-like responses in a way comparable to T lymphocytes [14], and some subsets are specialized to produce the Th17 cytokine IL-22 [15] although their features are not always comparable to NK cells. These unique features of NK cells may be associated with mDC factors that drive NK activation, including the combination of stimuli required for PRR and the cytokines that act in conjunction with inhibitory/activating ligands on NK receptors [16]. This review collates recent advances in the innate molecules and pathways related to mDC-mediated NK activation.

Direct or Secondary Activation of NK Cells by Microbial Patterns

DC/Mf as well as stromal cells express a variety of PRRs. In infection, these non-NK cell-derived mediators play a role in NK cell responses to pathogens [17]. Activation of these cells in response to PAMP can also lead to indirect NK activation which is mediated by affected accessory cells with altered membrane-associated molecules [16, 17]. Both soluble factors and membrane molecules join NK cell activation. Several reviews mention the mode of direct and accessory cell-derived (secondary) NK activation [2, 8, 16]. We just summarized this issue to facilitate the introduction of mDC/Mf-mediated NK cell activation.

Pathogen molecules often interact with NK receptors. Examples of direct pathogen interaction with NK cells have been demonstrated in mouse cytomegalovirus, whose m157 molecule interacts with Ly49H, an NK cell-activating/inhibitory receptor [18]. Influenza virus hemaglutinins bind the NKp46 of human NK cells [19]. Besides these NK receptor-interacting molecules, several kinds of bacteria/viruses are known to directly activate NK cells by PRR stimulation. Examples of microbial ligands for Toll-like receptors (TLRs) present in the NK cell membrane are as follows. Measles virus H protein interacts with TLR2 [20]. Mycobacteria muramyl dipeptides activate TLR2 residing on the NK cell membrane [21]. *Plasmodium falciparum* has an unidentified factor that interacts with TLR2/4 [22]. Some leishmania species have a lipophosphoglycan to bind to TLR2 [23]. Pam2 lipopeptides of a variety of bacteria serve as TLR2 ligands [24]. These factors also interact with mDC/Mf TLRs. Which TLRs in NK cells or accessory cells are more important for triggering NK cell activation in vivo should be an issue to be clarified.

Overview of the mDC Pattern Sensing System

mDC, which comprise many subsets [including bone marrow-derived DC (BMDC) and CD8α+ DC], possess subset-specific pattern-recognition systems. TLR, NOD-like receptors, and RIG-I-like receptors (RLR) are representative PRRs. The PRR repertoire in mDC has been described previously [17]. Two adaptors, i.e. MyD88 and TICAM-1 (TRIF), critically determine the signal pathways for TLRs, whereas interferon-β promoter stimulator 1 (IPS-1) (Cardif, MAVS, VISA) is the only adaptor that governs MDA5/RIG-I signaling (fig. 1). These adaptors are engaged in type I IFN induction and NK activation via partly overlapped but distinct pathways in a cell type-specific manner. Here, we summarize the signal pathways for TLR and RLR relevant to NK activation.

Signaling Pathways That Operate through the MyD88 Adaptor

MyD88 is the most common adaptor in the TLR and interleukin (IL)-1R signaling pathways [25, 26]. With the

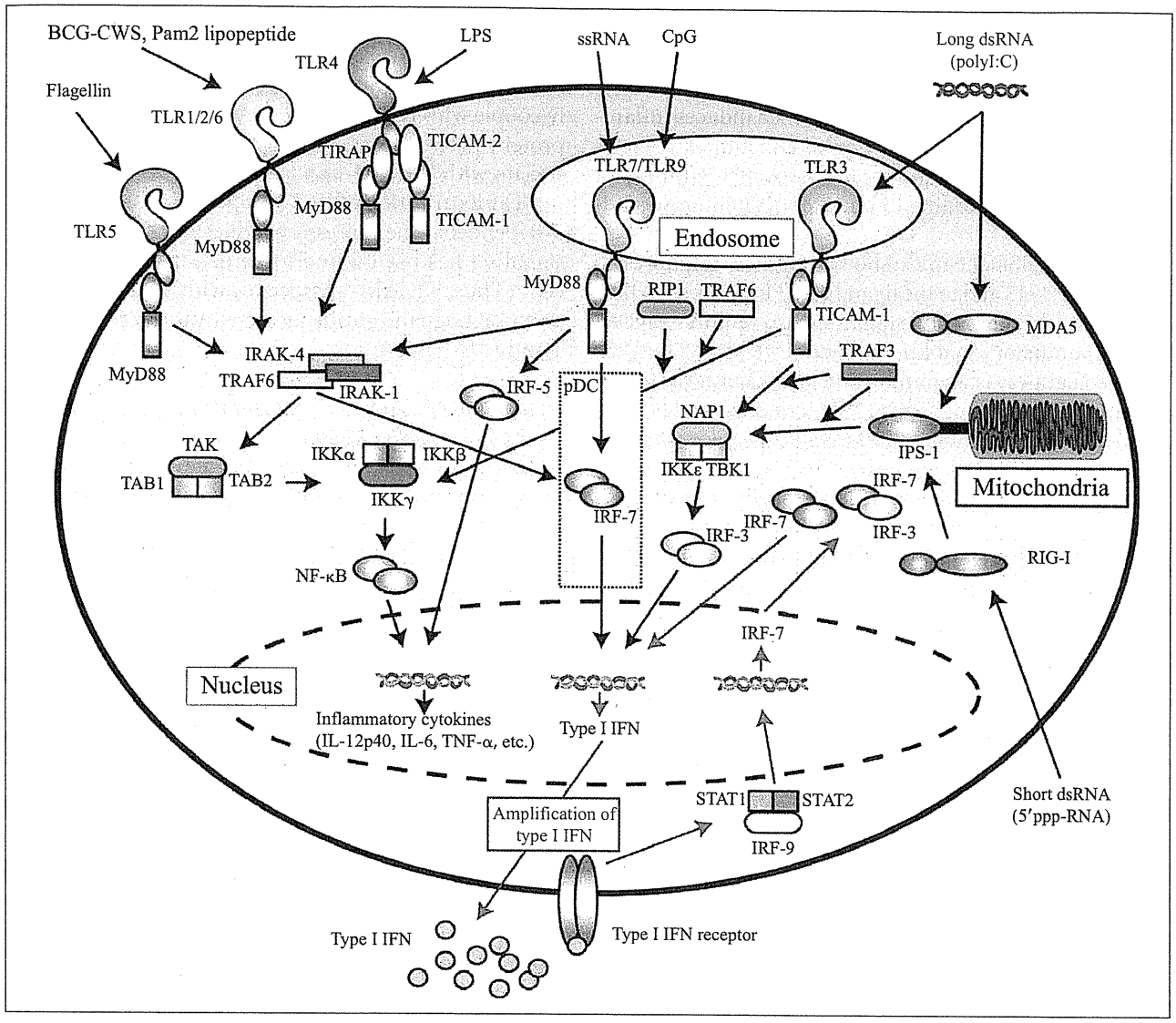

Fig. 1. TLR pattern-sensing system and cytoplasmic dsRNA recognition pathways. The TLR and RLR pattern-sensing systems involved in type I IFN induction and NK cell activation are depicted in a single cell model. pDC has a unique MyD88 pathway which is highlighted in the open square. All pathways except this MyD88 pathway function in BMDC of mouse and monocyte-derived DC of humans. Mouse spleen DC and human BDCA1/3-positive DC have weak potential for recognition of cytoplasmic dsRNA, reflecting a relatively immature feature of DC. Once TLR3 or TLR4 is stimulated, it transiently recruits TICAM-1 to form multimers. Subsequently, liberated TICAM-1 form a molecular complex named 'speckle' which serves as a nest for IRF-3/7 activation. In contrast, IPS-1 binds the outer membrane of mitochondria and forms an IRF-3/7-activating complex on the membrane. Once type I IFN is liberated, type I IFN production is amplified via the IFNAR pathway. NK cell activation occurs not only by soluble factors but also membrane proteins induced secondary to IRF-3 activation.

exception of TLR3, all TLRs in mice and humans can couple with MyD88. Only the MyD88 in plasmacytoid DC (pDC) is linked to IFN-induced signaling [27]. In pDC, TLR7/9 recruit MyD88 and the IRAK4/IRAK1 complex, allowing the phosphorylation of IRAK1 [28]. Activated IRAK1 forms a molecular complex with TRAF6/TRAF3/Osteopontin and IKKα. After forming a complex with MyD88, activated IKKα activates nearby IFN regulatory factor (IRF)-7 which, in turn, is dimerized and translocated to the nucleus [29]. The IRF-7 di-